

• U

C •

FCTUC

FACULDADE DE CIÊNCIAS

E TECNOLOGIA

UNIVERSIDADE DE COIMBRA

DEPARTAMENTO DE  
ENGENHARIA MECÂNICA

## **Design and implementation of a low cost hand for prosthetic applications**

Submitted in Partial Fulfilment of the Requirements for the Degree of Master in  
Mechanical Engineering in the speciality of Production and Project

### **Author**

**Andriy Sayuk**

### **Advisors**

**Prof. Dr. Mahmoud Tavakoli**

**Prof. Dr. Pedro Neto**

### **Jury**

#### **President**

**Professor Doutor Cristóvão Silva**

**Professor da Universidade de Coimbra**

**Professor Doutor Nuno Alberto Marques Mendes**

**Professor Auxiliar Convidado da Universidade de Coimbra**

**Professor Doutor Mahmoud Tavakoli**

**Investigador da Universidade de Coimbra**

#### **Advisors**

**Professor Doutor Mahmoud Tavakoli**

**Investigador da Universidade de Coimbra**

**Professor Doutor Pedro Neto**

**Professor da Universidade de Coimbra**

### **Institutional Collaboration**



**Institute of Systems and Robotics of the University of Coimbra**

**Coimbra, September, 2015**



## ACKNOWLEDGEMENTS

Working on this project was an exceptional experience. It was a long run and a lot of mistakes was made and many lessons were learned along this path. However I didn't completed it just by myself. It would be impossible to me to complete this work without support of some people.

Thus I would like to express my especial gratitude to:

Professor Doctor Mahmoud Tavakoli for the given opportunity to be involved in such remarkable project. His constant guidance and assistance were essential for this work.

Professor Doctor Pedro Neto for presenting me to Prof. Dr. Mahmoud Tavakoli as well as for all help given and encouragement during all the path.

I thank my fellow labmates for helping me to make first steps on this development process and for all their contributions to this work.

Also I want to express my gratitude to my sweetheart for being so patient with me, for a constantly supporting me and for giving me always what I needed most.

And at last but not the least, I would like to thank my family for their love and for supporting during all my academic path all my life in general - both spiritually and materially. Moreover, for everything...

Thank you!



## Abstract

The main goal for this work is to develop a body-powered prosthetic hand destined for an 8-year old boy with a congenital hand disorder. The fingers on his right hand are missing but the wrist movement had maintained.

Advancements in computer-aided design and additive manufacturing have opened new possibilities of designing and manufacturing prosthetic hands and other assistive devices at very low cost. People from recently formed community e-Nable Group started to use those advancements in order to design and deliver the prosthetic hand devices free of charge for anyone in need. The concept behind these hands is that no actuator is incorporated. The movement of the fingers is based on the movement of the wrist or the elbow. This makes the hands low cost, light-weight, and simple to control, the considerable features for the child prosthetic. So, the methodology for the present study is to use the e-Nable concept and create a hand that clearly outperforms the state of the art e-Nable hands in terms of grasping.

This dissertation starts with an overview about the currently existing upper-limb prosthetic devices and their categorization by their working principle. Then it shows a way that was passed from the conception up to the final version of the developed device identifying the problems that were faced in a process and solutions that were found for them. The idea of introducing fingers with compliant joint is also explained. Despite many advantages of compliant digits, their disadvantage is undesired lateral deflections. The way how this problem is addressed is shown in the end of this work.

Finally, there is an overview of all the achievements along with some future plans for further investigation.

**Keywords** Prosthetics, Body-powered, 3D Printing, e-Nabled, Compliant mechanisms.

---



## Contents

LIST OF FIGURES .....	ix
LIST OF TABLES.....	xi
SIMBOLOGY AND ACRONYMS .....	xiii
Simbology.....	xiii
Acronyms.....	xiii
1. INTRODUCTION .....	1
1.1. Motivation and required attributes.....	2
1.1.1. Light weight.....	2
1.1.2. Low cost .....	2
1.1.3. Intuitive control .....	3
1.2. Goal and Methodology .....	3
1.2.1. E-Nable Group.....	4
1.2.2. Methodology and Contributions.....	5
2. State-of-the-art.....	7
2.1. Upper-limb prosthetic devices .....	7
2.1.1. Electric-powered (Myoelectric) devices.....	7
2.1.2. Body-Powered devices .....	8
2.2. Additive Manufacturing role in evolution of low cost bionic hands .....	9
2.3. Compliant mechanisms.....	11
3. Development process.....	13
3.1. E-Nable body powered concept.....	13
3.1.1. Design, materials and fabrication methods.....	13
3.1.2. Testing the device.....	15
3.1.3. Preliminary findings (Problems) .....	16
3.2. First prototype.....	18
3.2.1. Development and manufacturing.....	18
3.2.2. Testing and results.....	21
3.3. Final version.....	23
3.3.1. Development and manufacturing methods .....	23
3.3.2. Testing and results.....	25
3.3.3. Performance comparison .....	26
4. Compliant joints with rigid materials .....	29
4.1. Problem .....	29
4.2. Compliant joints.....	31
4.2.1. Compliant materials - shape deposition modelling .....	31
4.2.2. Reinforced joints.....	33
4.3. Flexible joints through geometrical features on rigid materials .....	34
4.3.1. Design and simulations.....	35
4.3.2. Experimental setup .....	38

4.4.	Results and discussion .....	39
4.4.1.	Simulation results .....	40
4.4.2.	Experimental results .....	42
4.5.	Creation of the hand's digits .....	44
5.	CONCLUSIONS .....	47
5.1.	General conclusions .....	47
5.2.	Future works .....	47
5.3.	Publications .....	48
	BIBLIOGRAPHY .....	49
	APPENDIX .....	53
A1	. Palm Drawing .....	53
A2	. Gauntlet drawing .....	54
A3	. Finger drawing .....	55
A4	. Finger connector drawing .....	56
A5	. Detailed representations of grasps performed by <i>Soft-Enabled Hand</i> .....	57

## LIST OF FIGURES

Figure 1.1 – A photo of two hands of 8-year old boy. Left hand is normal and right hand has a congenital disorder .....	4
Figure 2.1 - Hosmer® Model 5 Hook - Adult Size .....	8
Figure 2.2 - Single-Cable System Hand by Otto Bock® with and without a cosmetic glove .....	9
Figure 2.3 - Dextrus Hand, an open source low cost prosthetic hand developed by Open Hand Project .....	10
Figure 2.4 -e-Nabled hands (from left to right): Raptor Hand, Cyborg Beast and Raptor Reloaded.....	10
Figure 2.5 - Flexy-hand 2 by Gyrobot .....	11
Figure 3.1 3D printed prosthetic Hand (Cyborg Beast). A: Top view (A1: Tensioner dial, A2: Lift nylon cords, A3: Chicago screws, A4: Tension balance system) and B: Bottom view (B1: Forearm adjustable Velcro strap, B2: Hand adjustable Velcro strap). ( <a href="http://www.cyborgbeast.com">www.cyborgbeast.com</a> ) .....	13
Figure 3.2 - 3D model of a palm and a gauntlet and 3d scanned model of receivers hand .	14
Figure 3.3 – Fully assembled test model: Cyborg Beast hand with reinforced gauntlet ....	15
Figure 3.4 – “Pick and Hold” test.....	15
Figure 3.5 - Tensioner problem at the first prototype.....	16
Figure 3.6 – Deformation process of the Velcro connection at the palm from the moment when it is totally open (“a”) to its partial closing (“b” and “c”).....	17
Figure 3.7 - Positions of the thumb. The thumb can be either abducted or adducted. In the abducted position the thumb is able to oppose the fingertips. The adducted position allows to either apply forces on the side of the fingers or it moves the finger “out of the way”. (This figure was adapted from [38]) .....	17
Figure 3.8 - 3D model of a modular prosthetic device composed by the gauntlet (1), a palm (2), finger connector (3), proximal phalange (4), distal phalange (5) and tensioning system (6).....	19
Figure 3.9 – Thumb position of a new palm (grey) compared to “Cyborg Best” palm (black).....	20
Figure 3.10 - Tensioning system consists of three parts: an outside box (1), a whippletree(2) and a thumb tensioner pin (3) .....	21
Figure 3.11 – 3D printed parts threatred with an industrial acetone before assembling .....	22
Figure 3.12 - Finger cots and rubber band were applied for more stable grasps.....	23
Figure 3.13 - An assembled prototype model worn by the recipient .....	23

---

Figure 3.14 - 3D model of a palm designed for the final version and the mold created for casting a Vytaflex® resin.....	24
Figure 3.15 - A fully assembled final version of the prosthetic device.....	25
Figure 3.16 - Text written with a pen holded by a prosthetic hand.....	25
Figure 3.17 - A variety objects possible to hold with a hand.....	26
Figure 3.18 - Grasp Taxonomy table by Felix et al. [38] .....	27
Figure 4.1 - The ISR-Softhand grasping a spherical object. The exerted forces to the thumb, cause undesired deflections on the compliant joint of the thumb, which affects the grasp stability in some cases. For heavier objects the grasp will be impossible, even if the thumb can exert enough normal force. ....	29
Figure 4.2 - Forces applied to the fingers in a tip pinch.....	32
Figure 4.3 - Model of the joint bending .....	32
Figure 4.4 - A thin rigid part is integrated to the thumb's flexible joint in order to increase the thumb's lateral stiffness .....	34
Figure 4.5 - Different joint models used for tests .....	36
Figure 4.6 - Geometry used in circular pattern joints D, E H (left) and G (right) .....	36
Figure 4.7 - Three types of loads analysed during FEA, maximum bending (top left), lateral deflection (top right) and displacement due to torsion (bottom).....	37
Figure 4.8 - A model of an example finger for a tests.....	38
Figure 4.9 - Experimental setup for measuring an undesired deflection.....	39
Figure 4.10 - Displacement visualization after FEA for lateral displacement. A - initial position, B - final position.....	40
Figure 4.11 Displacement visualization after FEA for torsion. A - initial position, B - final position.....	40
Figure 4.12 – Von Miss equivalent for stress distribution in each joint after FEA of applying a load $F_1 = 0,8N$ for maximum bending test.....	42
Figure 4.13 - Comparison between the results for "LD/FL" obtained by FEA and experimental methods .....	44
Figure 4.14 - Fabrication of a compliant finger, a 3D printed endoskeleton inserted into the designed mold which then filled with a silicone resin .....	45

## LIST OF TABLES

Table 1.1 - An average hand weight for different body weights .....	2
Table 2.1 - Commercially available myoelectric hands .....	8
Table 3.1 - Results for grasping tests for first prototype .....	16
Table 3.2 - Abstract of main problems and respective causes for the “Cyborg Beast” hand as well as their possible solutions.....	18
Table 3.3 - List of objects used for grasp tests with respectful specifications .....	27
Table 3.4 - An abstract of grasp tests results with quantity of possible, approximate and impossible to perform by the Cyborg Beast hand and the Soft-enabled hand .....	28
Table 4.1 - Comparison between the $\sigma_y/E$ ratio of 3D printed materials [49].....	37
Table 4.2 - Simulation results, the lateral deflection is measured after applying a constant force of 4N (F2) on all samples. The right column shows the total displacement on the tip of fingers after application of a torsional torque (M) of 0,12N.m.....	41
Table 4.3 - Simulation results, 2nd column shows maximum bending displacement, 3rd shows a ratio between lateral deflection (LD) and displacement due to flexion (FL) and 3rd column shows a ratio between displacement due to torsion (Tor) and FL .....	41
Table 4.4 - Simulation results, maximum stress value for each type load .....	41
Table 4.5 - Experimental results for undesirable deflection.....	42
Table 4.6 - Desired displacement, the ratios between lateral deflection (LD) and displacement due to flection (FL) and the ratios between displacement due to torsion (Tor) and FL. All ratios were calculated using the results of displacement values for higher masses, m2 and m4.....	43



## SIMBOLOGY AND ACRONYMS

### Simbology

$\delta$  – Deflection

$\sigma_y$  – Yield Strength

$E$  – Young`s modulus

$F_f$  – Tangential force

$F_n$  – Normal force

$I$  – Inertia

### Acronyms

3D – Three-Dimensional

ABS – Acrylonitrile Butadiene Styrene

CAD – Computer Aided Design

DEM – Departamento de Engenharia Mecânica

DOF – Degrees Of Freedom

FCTUC – Faculdade de Ciências e Tecnologia da Universidade de Coimbra

FEA – Finite Element Analysis

FDM – Fused Deposition Modelling

ISR – Institute of Sistems e Robotics

MEMS – Micro-Electro-Mechanical Systems

PLA – Polylactic acid

PVC – Polyvinyl chloride

SLA – Stereolithography

SLS – Selective Laser Sintering

TD – Terminal Device



## 1. INTRODUCTION

When a person becomes a limb amputee, he or she is faced with staggering emotional and financial lifestyle changes. It changes the quality of life radically by reducing such abilities as reaching, grasping, sensing through the sense of touch or gesture communication. Prosthetic devices may reduce those effects and make a life of this person easier. A prosthetic device can be defined as an artificial extension that replaces a missing body part such as an upper or lower body extremity. An artificial limb is a type of prosthesis that replaces a missing extremity, such as arms (upper limb prosthesis) or legs (lower limb prosthetics).

When a person decides to use a prosthetic device, the choice of the type of the prosthetic device is an important decision that an amputee should take: a cosmetic one, a body-powered or electric powered. Each of these categories have some advantages and disadvantages that should be considered. Too much weight, too expensive, too ugly or device too difficult to learn to deal with – those are the most common reasons why people give up using their prosthetic device. That is why the main focus of this work will be to develop a prosthesis that offers a good trade-off between different features to satisfy users in general and our volunteer in particular.

The volunteer who tests this hand is an 8-year old boy, who was born without fingers on his right hand. In this case requirements of the hand should be: low cost, light weight and easily operable and good looking device. While of these requirements are also valid for adult users, in case of amputee kids these issues are more sensitive. Complexity of control and heavy devices should be avoided. Furthermore the issue of the cost is even more important for kids, since they rapidly outgrow the prosthetic terminal.

This work starts by addressing the theme and its relevance. It introduces the main goal of the research work and methodology of its accomplishment. Chapter 2 gives an overview about the currently existing upper-limb prosthetic devices and their categorization by their working principle, Chapter 3 reveals the design and development of the prosthetic device that we developed including the fabrication methods, the problems that were faced and their solutions. Is also explained why introducing of the soft fingers with compliant joint is beneficial. Despite many advantages of compliant digits, their

disadvantage is undesired lateral deflections. In the 4<sup>th</sup> chapter we address this problem by performing Finite Element Analysis on different designs of compliant 3D printed joints in order to find out the most appropriate design. Chapter 5 summarizes the results and concludes the dissertation.

## 1.1. Motivation and required attributes

Over the last few decades there have been great advances in a development of prosthetic hands and terminal devices. Latest technological advances move towards more dexterous and realistic hand devices. However, the good combination of high functionality, durability, adequate cosmetic appearance and affordability is still rare to find.

### 1.1.1. Light weight

Final weight of a prosthesis is critical to the success of any prosthetic fitting. A human hand weights in average 0.585% of a total body weight [1]. Using this average, a hand weight was calculated for several body weights. The results can be observed at the Table 1.1.

**Table 1.1 - An average hand weight for different body weights**

Body weight, kg	Hand weight, kg	Hand weight, g
40	0,234	234
50	0,2925	292,5
60	0,351	351
70	0,4095	409,5

A recent internet survey of myoelectric prosthetic users concluded that 79% considered that their device was “too heavy”[2] even when its weight is close to the weight of a human hand. The reason for this is that the attachment methods between the prosthesis and the user compound the effects of weight in the terminal device. Therefore, the artificial hands need to be as light as possible or else they will end up in a closet.

### 1.1.2. Low cost

A typical prosthetic hand price range goes from several hundred to several thousand Euros. The cost is increased due to the materials used, the sophisticated actuators and the advanced sensing elements. Not every person can effort this range of expense. Moreover, in recent studies[3] most amputees confessed that the fear of damaging the

prosthesis terminal, forces them to avoid to use it on a daily basis or for difficult/dangerous tasks.

Special attention to the cost should be given for the child prostheses. Because children are continually growing, the size and shape of their residual limb is always changing. During the study at[4], researchers observed that the frequency of maintenance of myoelectric prosthesis can reach up to eight times per year. It can be costly to keep the child fitted with an appropriate device, but it's important because an ill-fitting device can cause discomfort and injury.

### **1.1.3. Intuitive control**

High cost is not the only obstacle that a myoelectric prosthesis user needs to overcome. An intuitive control is a highly desirable feature of a prosthetic device. As was reported in [5] and [6], twenty to forty percent of the people with an arm amputation do not use a prosthesis in daily living because lack of sufficient appropriate training. In many cases and due to the complicated control of the prosthetic terminal which is not very intuitive in most cases, such training can be long and complicated. No clear norm exists how much training is needed to handle a prosthesis [7], as it also proved in [8] “prosthetic users may differ in learning capability”. Minimizing a necessity for such trainings will make the idea to use a prosthetic device more attractive, especially for children.

## **1.2. Goal and Methodology**

Goal for this work will be to develop a fully functional body powered, low-cost, prosthetic hand device and customize it for an 8-year old boy with a congenital right hand disorder. All his fingers at right hand but a thumb are missing and the thumb has an abnormal shape due to unsuccessful surgeries that intended to implant a thumb as can be seen at Figure 1.1. Grasping possibility with such condition is really thinned out, that affects significantly the boy's quality of life.

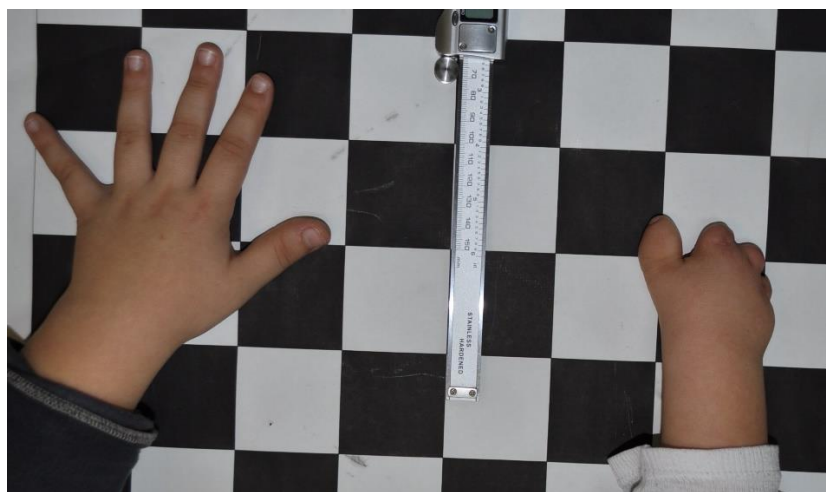


**Figure 1.1 – A photo of two hands of 8-year old boy. Left hand is normal and right hand has a congenital disorder**

### **1.2.1. E-Nable Group**

The developing process of the prosthesis will be based on a concept used by a e-Nable Group[9]. This is a rapidly growing worldwide community of over 3600 members collaborating to make free prosthetic hands using a 3D printing technology. They have created several open source 3D printable designs for low-cost body-powered prosthetic hands and are building it free of charge for anyone in need. The actual bill of material cost of making one of these hands is between 20-50 Euros. The concept behind these hands is that no actuator is incorporated. The movement of the fingers is based on the movement of the wrist or the elbow. There is no need for actuators, thus there is no need for controller and electromyography sensors. This makes the hands low cost, light-weight, and simple to control. The effort of the community is to make these hands as efficient of possible, while keeping it simple and without external actuators. In this dissertation we would make an important step toward a “soft-enable” hand that clearly outperforms the state of the art enable hands in terms of grasping.

E-Nable is a very recent community. First hand design was made at 2011[10] and after some time a community was created (page history starts at January, 2014[9]). Currently there are nine prosthesis designs available at the website for download. Most of them are made for hands which had kept wrist movement like the hand showed at Figure 1.1. Some e-Nable designs will be shown at the Chapter 2 of this work.

### **1.2.2. Methodology and Contributions**

Looking for the most popular e-Nable hand designs, we found out that there is some room for improvements. The objective is to increase the number of possible grasps, by changing the thumb's position, introducing compliant mechanism and adding new materials to the fabrication methods of the device in order to improve functionality of existing models.

So, the first step of this research work will be to choose and fabricate an existing model from the open-source designs available at the community's website [9] in order to study its performance and learn about its shortcomings and plan the improvements. The second version of the hand will be available to the community as an open source downloadable project.

The main contribution of course relies on the development of compliant fingers that are not only beneficial for e-Nable hands, but also for actuated prosthetic hands and industrial grasping units. But compared to traditional revolute joints, flexural joints suffer from a problem which is related with the deflections and torsions in the undesired directions. We therefore made another analysis with finite element simulations on the geometry of a 3D printed flexural joint to make the best trade-off between the required bending force, and undesired lateral deflections, taking into consideration also the maximum localized stress in the parts.



## 2. STATE-OF-THE-ART

### 2.1. Upper-limb prosthetic devices

All prosthetic devices can be separated into two groups: passive devices (cosmetic) and active devices (functional). A passive prosthesis provides the patient with a visual replacement for their absence without providing any additional functionality. Passive, or cosmetic, prostheses are primarily constructed from flexible latex, rigid PVC, or silicone. Each device is customized to best match their user's skin tone. There are some advantages why some users can choose a passive device. As a non-functional device, passive prostheses are normally durable, rugged, and lightweight.

An active prostheses can be Electric-powered, body-powered or mixed. Each of them has its own advantages and disadvantages.

#### 2.1.1. Electric-powered (Myoelectric) devices

Myoelectric prostheses creates a movement based on electrical charges that naturally occur during muscle activation. Electrodes are placed on the surface of the muscle flexor and extensor to detect the electrical output. The outputs range from 5-200 microvolts and are then amplified to control the hand which is equipped with one or several motors.

There are many brands of myoelectric hand prostheses on the market. BeBeoinic Hand[11] and I-Limb Hand[12] are two popular models, very similar between themselves. Each of this hand has five DC motors - one for each finger and one for the thumb flexion/extension. The thumb is brought manually into the desired position in both cases. Vincent Evolution 2 [13] hand uses one additional motor to control the thumb position. It also has a sensoring system located on the tip of the fingers that provides a feeling of touch and gripping force to the wearer. Michelangelo hand [14] is equipped with only two drive units. The main drive is responsible for gripping movements and gripping strength, while the second drive controls the thumb position. Actively driven components in this device are the thumb, index finger and middle finger. Some specification of devices mentioned above are shown at the Table 2.1.

**Table 2.1 - Commercially available myoelectric hands**

	<b>DOF</b>	<b>Number of actuators</b>	<b>Weight, g</b>	<b>Price [15], [16]</b>
<i>I-Limb Hand</i>	6	5	445-615	23000€
<i>BeBeoinic Hand</i>	6	5	495-539	16000€
<i>Vincent Evolution 2</i>	6	6	500	25000€
<i>Michelangelo Hand</i>	6	2	380	60000€

### 2.1.2. Body-Powered devices

Body powered prostheses are devices that move as a function of the user's aggregate body motion. Hands, forearms, and elbows all may be controlled by a system of harnesses attached to portions of the users' body that have maintained their natural movements. This type of prosthesis is very reliable and can be used in environments involving dust and water.

The advantages of body-powered prostheses include: simple operational mechanisms with intrinsic skeletal movement (which voluntarily opens/closes a terminal device) that doesn't require additional training to use, silent action, light weight, moderate cost, durability and reliability.

The voluntary opening split-hook (Figure 2.1) is widely accepted as the most commonly utilized functional terminal device in body-powered prosthetics [17]. Prosthetic hooks have proven to be an effective and reliable tool for amputees to use in their daily lives.

**Figure 2.1 - Hosmer® Model 5 Hook - Adult Size**

The weight of the device depends mostly on the size of the device and the material used (stainless steel, aluminium and titanium are the most common). Looking at the Hosmer® products, a worldwide prosthetic manufacturer, the hook weight ranges from 85g (Aluminium child size model) to 397g (Stainless Steel adult size) [18].

The average price for Hosmer hook is about 500\$[19].

“The System Hand” by Ottobock (Figure 2.2) is another example of commercially available body-powered terminal devices. It consists of three parts – the aluminium hand chassis with hand mechanism, the shaped inner hand, and the cosmetic glove which, together, provide both functionality and a natural appearance[20]. A hand can be voluntary opening (remain closed until pull on cable opens it) or voluntary closing (remain open until pulling on the cable closes it with a grip force proportional to the amount of force the person puts on the cable). The device’s control cable is connected to the harness system mentioned earlier on this chapter. Approximate weight of the device is 370g and it costs near 620€(price is just for TD)[15].

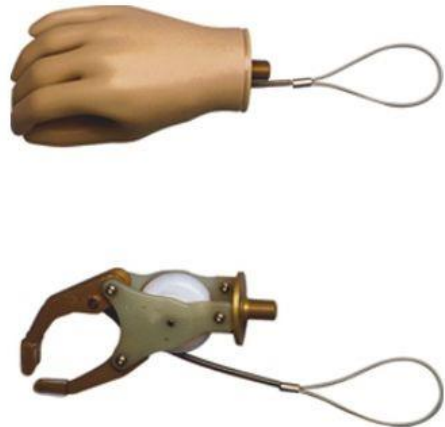
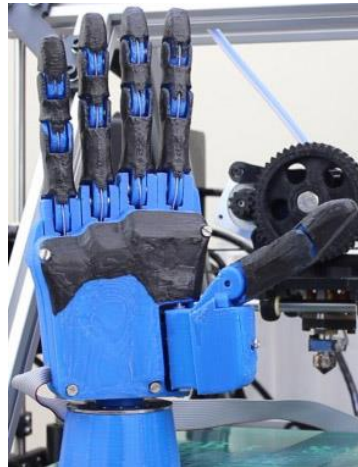


Figure 2.2 - Single-Cable System Hand by Otto Bock® with and without a cosmetic glove

## 2.2. Additive Manufacturing role in evolution of low cost bionic hands

Advancements in computer-aided design (CAD) and additive manufacturing have opened new possibilities of designing and manufacturing prosthetic hands and other assistive devices at very low cost [21]. Additive manufacturing provides the designer a great freedom on the design and optimization of the mechanisms. Furthermore it is low cost compared to traditional manufacturing techniques such as machining. It is also fast, thus a designer can make many iterations of design to reach an optimal functioning

prototype in a short time. The open-source myoelectric hands such as Dextrus hand[22], [23] (Figure 2.3), 6 DOF Hand developed at [24] or the iCub Hand [25] are successful examples of such research.



**Figure 2.3 - Dextrus Hand, an open source low cost prosthetic hand developed by Open Hand Project**

Another example of a recent development is the Cyborg beast: a low-cost 3d-printed prosthetic hand for children with upper-limb differences [26] in this hand “*Finger flexion is driven by non-elastic cords along palmar surface of each finger and is activated through 20-30° of wrist flexion*”[26]. It is actually one version of the e-Nable hand community. The materials used for 3D printing of Cyborg beast hand are polylactide (PLA) and acrylonitrile butadiene styrene (ABS). The weight of fully assembled hand is less than 200g and present cost of materials is about 50\$.



**Figure 2.4 -e-Nabled hands (from left to right): Raptor Hand, Cyborg Beast and Raptor Reloaded**

This model is one of the most popular hands built by e-Nabled community. Very similar to this, is the “Raptor Hand” and the most recent “Raptor Reloaded” (Figure 2.4). Another available model is showed on a Figure 2.5, “Flexy Hand 2” [27] which benefits from a more anthropomorphic look and uses a hinges made with flexible filament for finger joints.

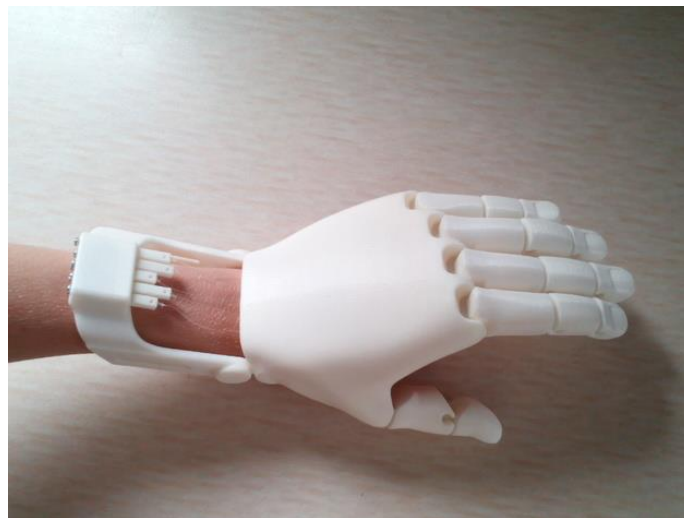


**Figure 2.5 - Flexy-hand 2 by Gyrobot**

### 2.3. Compliant mechanisms

Integration of the compliance into the robotic systems received an increasing attention in the robotics community during the recent years. Compliance can result in a passive adaptability in articulated arms or in grasping mechanisms. Integration of the compliance is also explored since it enhances the safety which is appreciated in the domain of the human-robot interaction.

One important subject of research in this domain is the creation of joints with a compliance behaviour. A compliant joint can be formed by a proper controller, e.g. by allowing a predefined tolerance from the target position in the position control loop. Within that tolerance domain the actuator can only apply a limited predefined torque. Yet this is not optimal for grasping applications due to problems such as control complexity, and control loop delays. The DLR HAND II [28] integrates the compliance into the control loop by using an appropriate impedance controller. Yet this solution demands for full hand actuation and a sophisticated controller.

Compliance can also be integrated in the actuator by integration of compliant elements i.e. springs to the system. For instance, in some tendon driven hands this was achieved by coupling a spring serially with the actuator. The so called Series Elastic Actuator (SEA), issued for instance in Meka-H2 compliant hand [29]. The under-actuated H2 hand has a total of 12 DOF controlled by 5 actuators. Each finger is driven by a Series Elastic Actuator by placing a spring between the motor and the tendon.

Another approach is to directly integrate compliance into the joints. Pisa-IIT Softhand[30], ISR-Softhand[31] and the UB hand[32] are examples of recent development of anthropomorphic hands that directly integrate the compliance into the joints. In Pisa-IIT Softhand several elements are interconnected with elastic elements, while in UB hand the joint compliance is achieved by integration of springs into the joints.

Flexirigid[33] and SDM hands[34] are examples of non-anthropomorphic grasping mechanisms that use elastic joints for a better adaptability to objects. In Flexirigid several rigid elements are connected together with an elastomer. In this approach elastic polymeric joints take place of the traditional revolute joints. Such elasticity helps in a high adaptability to a wide range of objects shape and size. In the SDM hand[34], and ISR-Softhand[31], rather than the revolute rigid joints, elastic joints were used. The elastic joints in these hands are formed by casting a urethane rubber into the molds that are built in the 3D printed parts.

### 3. DEVELOPMENT PROCESS

#### 3.1. E-Nable body powered concept

A concept already mentioned at Chapter 2 of this work, an open source 3D-printed prosthetic hand named “Cyborg Beast”[26], was taken as a base for developing the working prototype in this work(Figure 3.1). This hand is one of the most advanced models published at the community’s website [9] at the time. In a research performed by Creighton University [35] 34% of tested users of the “Cyborg Beast” hand (children from 3 to 16 years of age) reported a significant increase in quality of life, 58% had indicated a small increase and just 8% had no change in quality of life. So, despite the good user’s feedback, it shows that the hand design still has space for improvement and is a good choice to be a base for this research work.

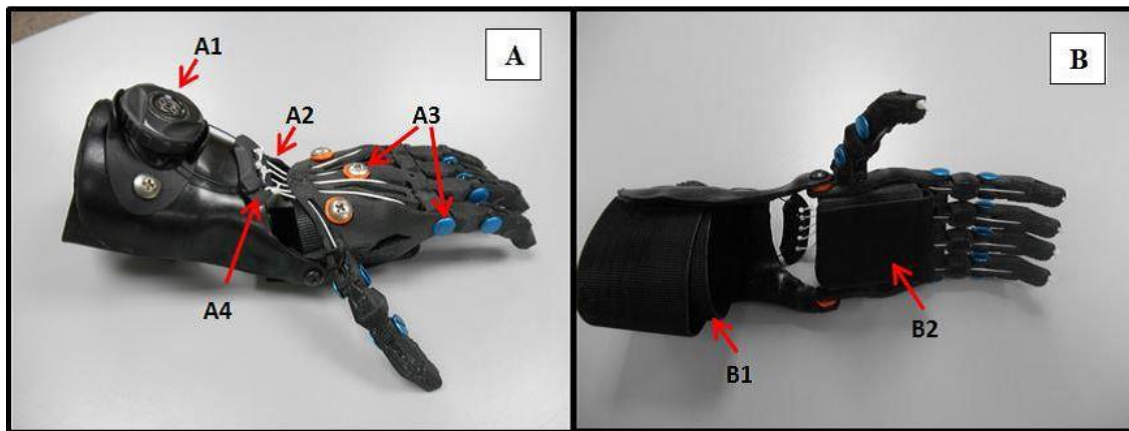


**Figure 3.1 3D printed prosthetic Hand (Cyborg Beast).** A: Top view (A1: Tensioner dial, A2: Lift nylon cords, A3: Chicago screws, A4: Tension balance system) and B: Bottom view (B1: Forearm adjustable Velcro strap, B2: Hand adjustable Velcro strap). ([www.cyborgbeas](http://www.cyborgbeas))

##### 3.1.1. Design, materials and fabrication methods

For the test model we used the design of the palm and fingers from a “Cyborg Beast” model with reinforced gauntlet version. The original design was created by Jorge Zuniga due to an increasing need for practical, easy-to-replace, aesthetically appealing low-cost prosthetic devices for children [36]. After successful tests 3D files were placed for free download at several web resources including an e-Nabled group [9].

As the first step, we asked the volunteer to come to our Institute and made a 3D scan of his hand with a 3D scanner device. We then imported the files into Solidworks software in order to design a patient specific design of the Gauntlet and the other parts of the hand. Usually in e-Nable community the scaling of the parts and sizing to the patient is achieved approximately. Here we decided to use 3D scanning in order to make more a model better fitted to the volunteers hand Figure 3.2.

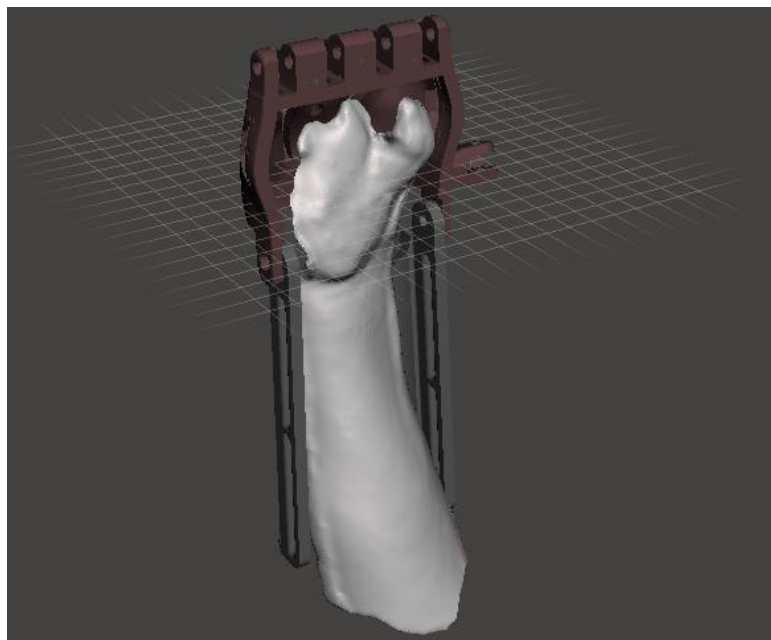


**Figure 3.2 - 3D model of a palm and a gauntlet and 3d scanned model of receivers hand**

After proper scaling the 3D printable parts were ready for manufacturing. An ABS plastic was used for the purpose. It represents better mechanical properties and higher temperature resistance than PLA plastic [37]. Distal and proximal phalanges were assembled together and joined to the palm using steel alloy shafts with diameter of 5mm. Elastic cords placed inside the dorsal aspect of the fingers provide passive finger extension. Finger flexion is provided by non-elastic cords along the palmar surface of each finger connected to the tension pins placed at the top of the gauntlet. A 10mm foam layer was placed at the inside part of the gauntlet and the palm to make an interface between the skin and the plastic. An adjustable Velcro straps were used to connect a prosthesis to an arm.

Fully assembled device is shown at Figure 3.3:



Figure 3.3 – Fully assembled test model: Cyborg Beast hand with reinforced gauntlet

### 3.1.2. Testing the device

A prosthesis was tested by performing several grasping operations: closing of an empty hand, picking and holding some objects - a glass, a candle, and a lemon among others (Figure 3.4).



Figure 3.4 – “Pick and Hold” test

For some objects it was possible hold if it was correctly placed into the prosthesis with aid of a healthy hand, for other, picking was possible but the object was slipping from the hand right after. That's why a "Pick and Hold" test was introduced. It consisted in picking an object from the table just with assistance of a prosthetic devise and verify if it is possible to hold it for period of time larger than 5 seconds. The summary of a "Pick and Hold" test is displayed at the Table 3.1

**Table 3.1 - Results for grasping tests for first prototype**

Object	Pick	Hold
Lemon	Yes	Yes
Pear	Yes	Yes
Glass	No	No
Candle	No	No

### **3.1.3. Preliminary findings (Problems)**

During the assembly was noticed that a tensioner mechanism (Figure 3.5, region "A") has some issues. A precise adjustments of driving cords through the tension pins was impossible. Because a size of the pins is relatively small, a precision of a 3D printer wasn't enough to make a mechanism work well.

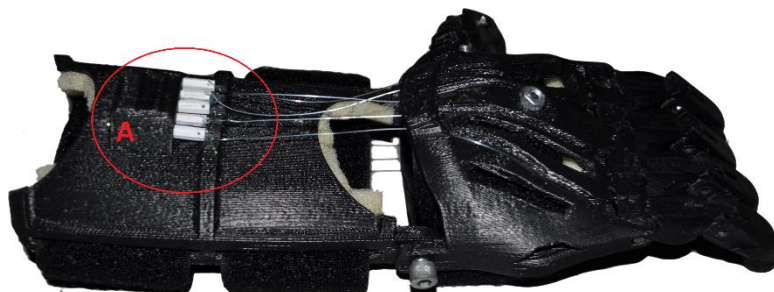


**Figure 3.5 - Tensioner problem at the first prototype**

The lack of friction between the prosthesis and objects at the contact points was creating some difficulties to pick and hold the object with the smooth surface. Thus to establish the necessary friction to avoid slippage of the parts, additional normal force is required which requires additional effort from the amputee. An absence of any rigid material at the bottom part of the palm makes the connection with the body too loose to transmit correctly the wrist movement responsible for finger bending to the palm part of prosthesis. As a consequence, it was hard to keep a tight grasp for a long period of time. Figure 3.6 demonstrates the amount of free wrist movement present on a Velcro

connection. After solving those problems less force will be required to perform firm and safe grasps.

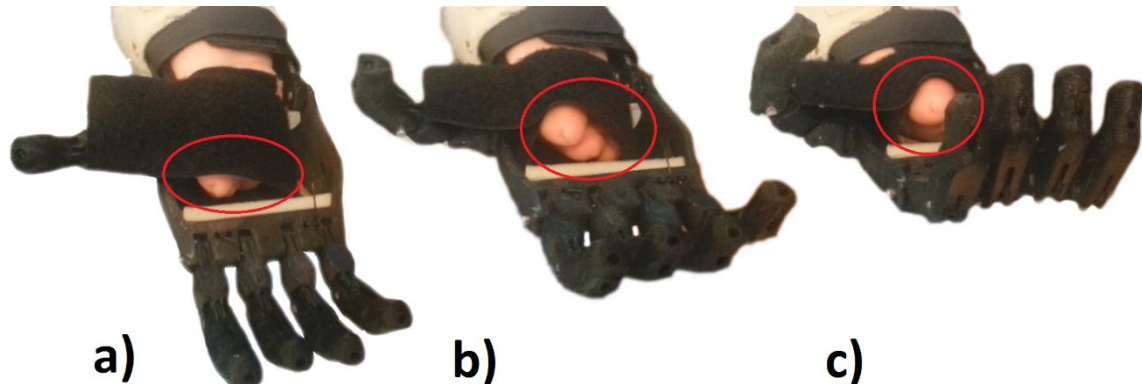


**Figure 3.6 – Deformation process of the Velcro connection at the palm from the moment when it is totally open (“a”) to its partial closing (“b” and “c”)**

The last, but not the less important matter was a thumb position and its orientation (Figure 3.7, right). In the original design, a thumb was positioned in adducted position. In recent studies [38] all known types of grasps were classified according to several parameters, including the position of the thumb. Only 10 (out of total 33 grasps) fits into “Thumb adducted” type, that means that positioning the thumb in abducted position will allow to perform a higher number grasps.



**Figure 3.7 - Positions of the thumb. The thumb can be either abducted or adducted. In the abducted position the thumb is able to oppose the fingertips. The adducted position allows to either apply forces on the side of the fingers or it moves the finger “out of the way”. (This figure was adapted from [38])**

## 3.2. First prototype

### 3.2.1. Development and manufacturing

For the first prototype, all structural design was drawn from scratch based on learnings from the test model. Table 3.2 resumes the main problems of e-Nabled body powered concept that was taken into the account during the developing of the new device.

**Table 3.2 - Abstract of main problems and respective causes for the “Cyborg Beast” hand as well as their possible solutions**

Problem	Cause	Solution
Many Grasps were not possible to perform	The opposition type grasps were not possible due to the fact that the position of the thumb was not correct	Correct the thumb's position and orientation
	Lack of contact point on the thumb	Add a rigid base in the palm as an additional contact point
	Lack of friction between grasping object and the device	Add a high friction silicon to the fingers and to the palm
High forces were required to close the hand	High friction between the tendons and the plastic surface.	Apply an acetone smoothing to the ABS surfaces
	An interface between the body and the device is to	Add a rigid base in the palm solves this problem
Elastic tendons were rupturing after some time of use	Fatigue	The new finger doesn't require elastic tendons

To ease a maintenance and future upgrades, was opted to adopt a modular structure. We decided to use the palm and the gauntlet as a basic structure and to keep an

opened possibility to add new finger designs and to use different tensioning systems. A full 3D model of the prosthesis is displayed at the Figure 3.8.

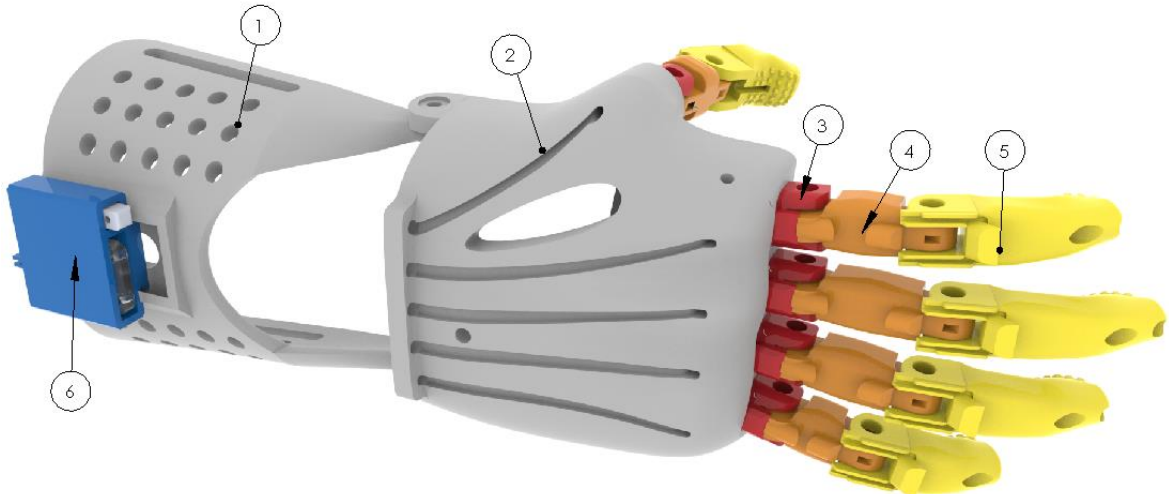


**Figure 3.8 - 3D model of a modular prosthetic device composed by the gauntlet (1), a palm (2), finger connector (3), proximal phalange (4), distal phalange (5) and tensioning system (6)**

The new hand was manufactured using the same 3D printing technology used for the fabrication of the test model. The surfaces were polished with industrial acetone then. This treatment grants to the surface a smooth and shiny finish that reduce the friction between the tendon cords and the palm surface and gives to the model a better look.

### 3.2.1.1. Palm and the gauntlet

The palm and the gauntlet were designed to follow the shape of recipient's arm, guiding by the photos taken previously. In order to reduce the overall mass of the device, some hole patterns were applied on a gauntlet and the palm.

Few new features were included to the palm design. The thumb socket was reoriented and was positioned in the "abducted position" (see Figure 3.7) at the bottom part of the palm where also a solid base was added. (Figure 3.9, top). Regarding the classification made in [38] this thumb position should allow more grasping options. Furthermore we designed a modular finger insertion box into the palm, which makes it easy to replace fingers in case of damage.

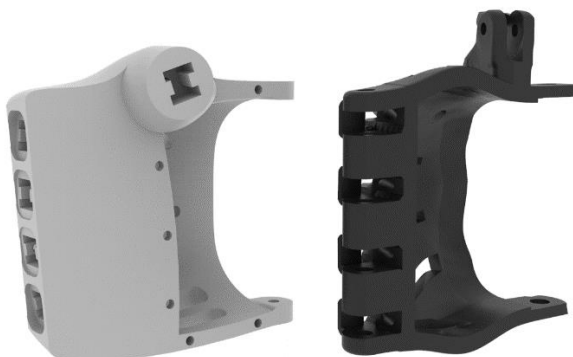


**Figure 3.9 – Thumb position of a new palm (grey) compared to “Cyborg Best” palm (black)**

Since a gauntlet from the test model broke after some time of use, this fact was taken in attention during the design of a new one. The new Gauntlet is shorter but more tolerant to forces (by increasing its thickness at the critical points). Decreasing its overall length reduces an applied moment when the force is applied, and also makes the device lighter.

### **3.2.1.2. Fingers**

Even though we planned for development and integration of compliant fingers for the final version of the device, we opted to test a temporary solution on the finger side based on the original “Cyborg Beast” fingers with slight changes. In this case we could evaluate the effect of each of the other changes independent from the finger’s changes. (i.e. the gauntlet, the position of the thumb and the effort required to close the hand) Each phalange was resized in order to keep a similar appearance to a human hand. (I.e. Pinkie should be the smallest, middle – the longest). The fingers are connected to the palm with assistance of the small connection parts (Figure 3.8, finger connector) which fits into the corresponding sockets at the palm.

### **3.2.1.3. Tensioning system**

A different tensioning system was introduced to the prosthesis design. It is based on designed by an e-Nable user Jason Bryant “Gripperbox 3.0” [39]. Few similar systems can be found at the state-of-the-art. The thumb is connected to the fixed tensioner pin (3), as shown in the Figure 3.10. Tendons from index and middle fingers are connected together and pass through the hole “C” of a suspended triangle, a whippetree (2). In the similar way tendons from ring and pinkie fingers are connected through another hole (“B”) of the whippetree. The triangle is fixed to the box (1) through a hole “A”. The power

transmitted from tendons is balanced between the fingers and they take on the shape of the object being held, thus makes the grip more secure. It provides an adaptive grip so that each finger in the hand will adjust to the shape of the object being held. In the other word, if one of the fingers contacts the object, the other fingers continue to close until they also make a contact with the object. In this way higher number of contacts is guaranteed.

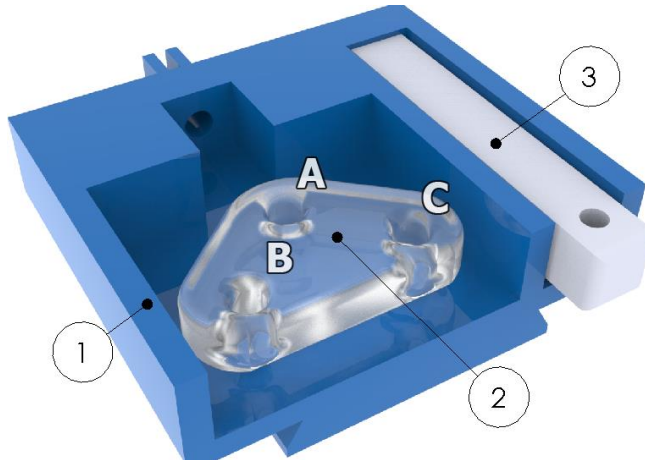


**Figure 3.10 - Tensioning system consists of three parts: an outside box (1), a whippetree(2) and a thumb tensioner pin (3)**

Like all previous parts of the prosthesis, the box and the pin and the whippetree were printed on a FDM 3D printer, but after some tests we decided to print a whippetree piece on a SLA 3D printer, since it provides a smoother surface finishing,

### 3.2.2. Testing and results

Since it was an intermediate prototype built with a purpose to test the introduced new features, some elements as the foam interface and the Velcro straps weren't applied on this model. At the Figure 3.11 3D printed fingers are shown before assembling them on an already mounted together palm and gauntlet.

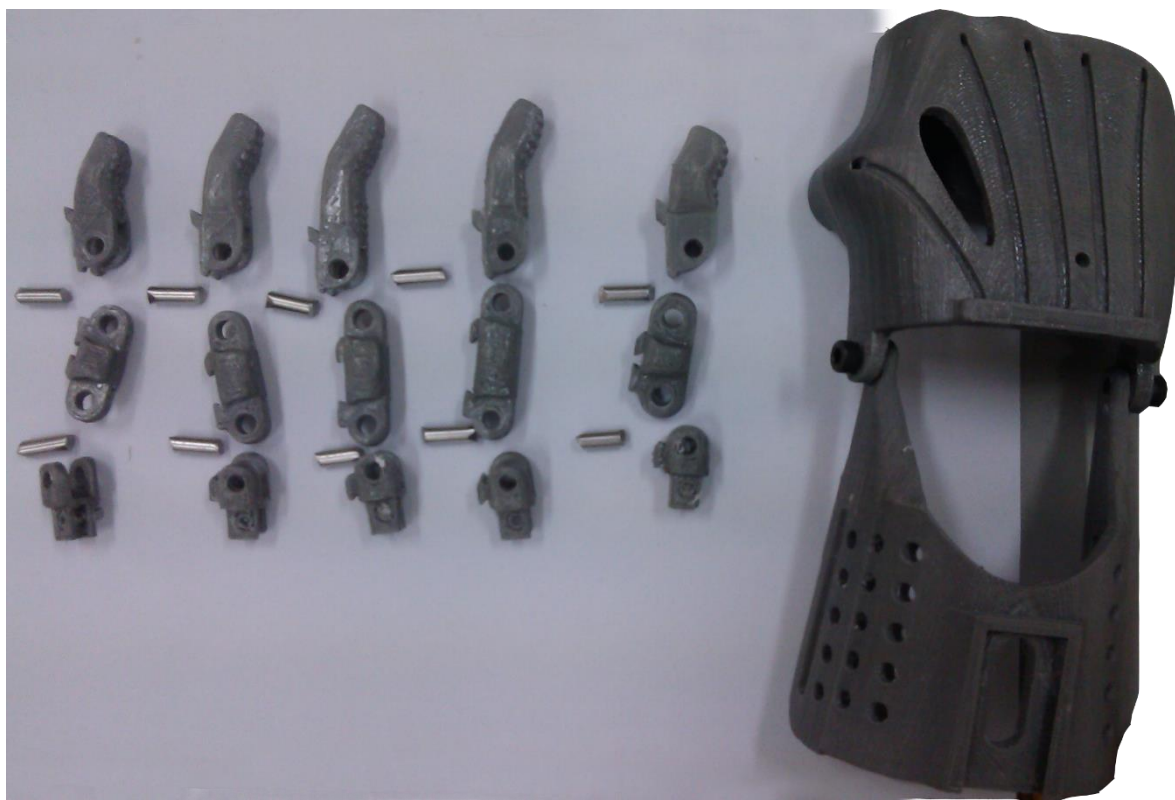


**Figure 3.11 – 3D printed parts treated with an industrial acetone before assembling**

Once assembled, the device was first tested in the lab conditions and after some tests was performed by the volunteer. The problem of low friction between the fingers and the objects maintained from the test model and was temporarily solved by applying the latex finger cots on device's fingers and the rubber bend at the bottom part of the palm as shown at the Figure 3.12 (left). The right part of the same figure shows a device holding a small bottle. To best of our knowledge such perfect grasp of the bottle was not possible by any of the previous e-Nable hands. Please note that the cylindrical grasp is the most used grasp type by humans during the daily tasks [40].



**Figure 3.12 - Finger cots and rubber band were applied for more stable grasps**

After successful lab tests the device was brought to the recipient. New shape matched exactly the shape of his arm as can be seen at the Figure 3.13. A new thumb orientation and the system for adaptive grasp had opened the possibilities to execute solid cylindrical and conoid grasps, impossible to perform with a previous hand, yet the device maintained an ability to perform spherical and hook types of grasp with improved stability.

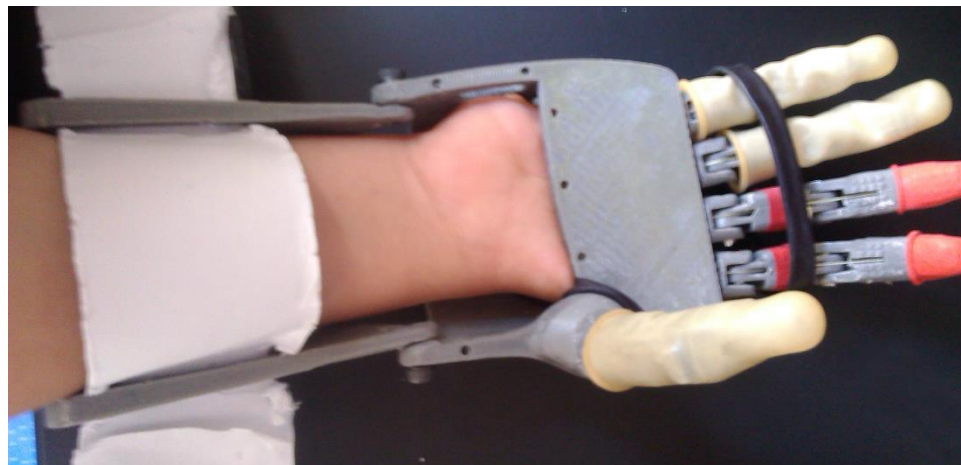


**Figure 3.13 - An assembled prototype model worn by the recipient**

### **3.3. Final version**

#### **3.3.1. Development and manufacturing methods**

As was observed with a previous prototype, adding a high friction material can improve significantly the grasping ability. Using a mold designed for the purpose, a urethane rubber compound (Vytaflex® 30) was casted at the bottom part of the palm,

which was slightly changed in order to increase the contact area between rigid and rubber parts of the palm and to provide a smooth transition between both (Figure 3.14).

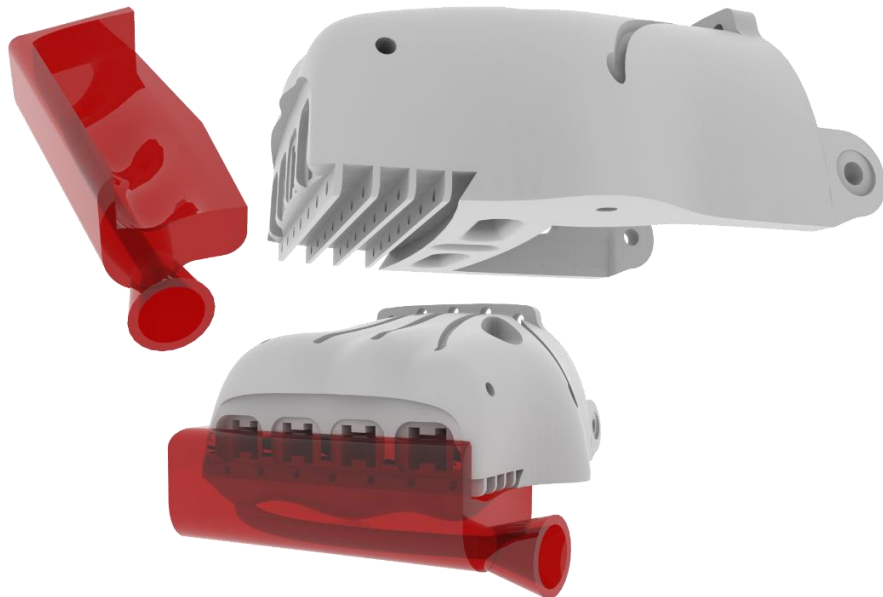


**Figure 3.14 - 3D model of a palm designed for the final version and the mold created for casting a Vytaflex® resin**

Implementation of the finger with a compliant joint was another upgrade for this version of the device. It provides a better grasp by creating a multiple contact points between a finger and an object. The process of development of the finger with a compliant joint will be described in more details in the Chapter 4 of this work.

Fingers were manufactured in two steps: an endoskeleton is produced using SLS 3D printing technology, then it was placed in a mold fabricated using SLA 3D printer, which has form close to the human finger but with some changes needed for better functionality of a finger and a resin is casted around the endoskeleton. The resin casted around the endoskeleton offers more stable grasps and gives to a finger the aspect closer to a human finger.

Different 3D printing technologies were used to seize the advantages of each to get the parts with desirable attributes. Models fabricated using SLS technology are strong and flexible as required for compliant fingers and SLA 3D printing provides good precision and smooth surface finishing, the attributes desirables in molds.

### 3.3.2. Testing and results

Once the resin was casted all device's parts were assembled together, weighed and the hand was ready for testing (Figure 3.15). The overall mass of the hand is 230g.

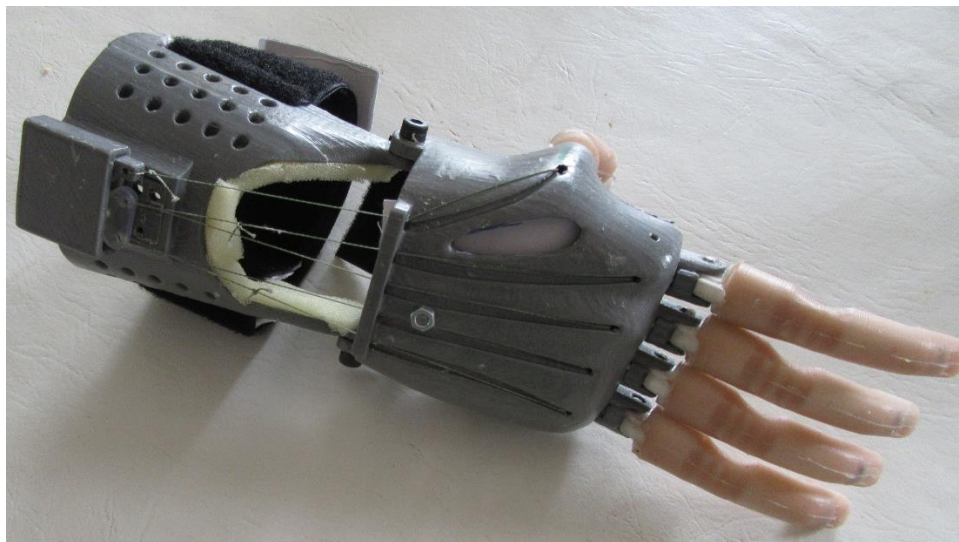


**Figure 3.15 - A fully assembled final version of the prosthetic device**

The final version of the prosthesis was tested in the lab conditions. Several grasps were performed on objects with different forms and weights in order to understand the capabilities of a hand. As can be seen from the Figure 3.17, a big variety of objects can be handled by a prosthesis. It is possible to use hand to move something, to perform simple operations like drinking a water from a glass or just for playing with toys without any experience of using a prosthetic device. With some training it may be possible to perform more complex operations like riding a bicycle or even writing (Figure 3.16)

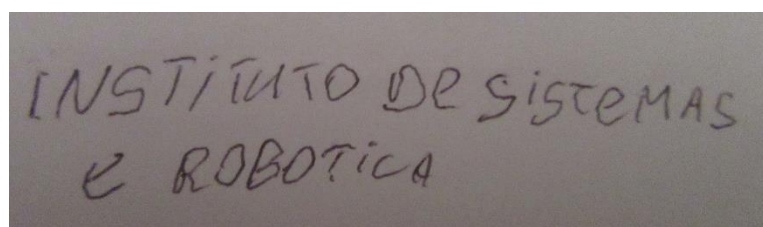


**Figure 3.16 - Text written with a pen held by a prosthetic hand**

Yet there is a weight limitation for the device. Objects heavier than 750g are difficult to hold for a long time and object with weight more than 1kg are impossible to lift.



**Figure 3.17 - A variety objects possible to hold with a hand**

### 3.3.3. Performance comparison

In order to create a benchmark that compares the performance of the “Cyborg Beast” and the “Soft-Enabled Hand”, both hands were tested by trying to perform each of 33 grasp from Grasp Taxonomy table by Felix et al. [38] (Figure 3.18).

It was possible to classify all the performed grasp into 3 categories: possible, approximate and impossible. By approximate are perceived grasps when the hand doesn't imitate perfectly the grasp scheme indicated on Grasp taxonomy table at [38], but which are still possible to perform. In other words, when it was possible to hold the object, but an anthropomorphic grasp imitation wasn't achieved.

Opposition Type:	Power					Intermediate			Precision					
	Palm		Pad			Side			Pad				Side	
	Virtual Finger 2:	3-5	2-5	2	2-3	2-4	2-5	2	3	3-4	2	2-3	2-4	2-5
Thumb Abd.														
Thumb Add.														

Figure 3.18 - Grasp Taxonomy table by Felix et al. [38]

To test each of 33 known grasp types 14 different object were used. Their diameter and mass are specified on the Table 3.3.

Table 3.3 - List of objects used for grasp tests with respectful specifications

Object	Diameter, mm	Mass, g
Tube	75	73
Tube2	35	192
Glass	58	115
Pen	10	10
Battery	14	23
CD	120	17
Tennis ball	65	61
Ping-pong ball	38	2
Plate	-	10
Scissors	-	-
Hex key	5	5
Sphere	59	5
Notebook	-	70

As it possible to visualise at the Table 3.4, the Soft-Enabled Hand clearly outperforms the Cyborg Beast in term of performance capable to perform the total of 23 grasp types against only 5 grasp type possible to perform with Cyborg Beast.

**Table 3.4 - An abstract of grasp tests results with quantity of possible, approximate and impossible to perform by the Cyborg Beast hand and the Soft-enabled hand**

Model	Imitation	Number of performed grasps	Grasp type
<i>Cyborg Beast</i>	Possible	2	15, 28
	Approximate	3	5, 9, 30
	Impossible	28	rest
<i>Soft-Enabled Hand</i>	Possible	17	1, 2, 3, 7, 8, 10, 11, 12, 13, 14, 18, 24, 25, 26, 27, 28, 33
	Approximate	6	5, 6, 15, 17, 19, 31
	Impossible	9	4, 16, 20, 21, 22, 23, 29, 30, 32

## 4. COMPLIANT JOINTS WITH RIGID MATERIALS

### 4.1. Problem

Despite the advantages of the soft joints in terms of safety, compliance and adaptability, they suffer from a common problem. That is, the undesired deflections and twisting in the joints in the direction perpendicular to the desired flexion axis. The flexibility of the joints makes them flexible in many directions. For instance, as can be seen in Figure 4.1 the joint compliance causes an undesired lateral deflection on the thumb of the ISR-Softhand [31].



**Figure 4.1 - The ISR-Softhand grasping a spherical object. The exerted forces to the thumb, cause undesired deflections on the compliant joint of the thumb, which affects the grasp stability in some cases. For heavier objects the grasp will be impossible, even if the thumb can exert enough normal force.**

To resolve this, some solutions were studied based on optimization of the flexible joints, hybrid joints based on integration of rigid parts and flexible parts, as well as studying the geometric features and deflection of rigid materials and thus developing compliant joints with rigid materials. In all cases it is desired to have minimum joint stiffness around one axis, and maximum stiffness on the other axes.

Compliant joints and Flexural joints have been widely considered in the precision control elements and also in the design of MEMS. However, they have not received enough attention in the other robotics community, probably because of their non-conventional nature, i.e. due to the difficulties in their design, optimization and fabrication.

However the last part of this chain, i.e. the fabrication is currently addressed by additive manufacturing methods. There are similarities between these joints and “flexure

bearings”, and thus this option will be investigated. Flexural joints have been mostly designed and optimized for development of MEMS [41], [42], since when exposed to external forces, their resulting pose can be precisely modelled. Their topology optimization however is mostly concentrating on the problem of distributing a limited amount of material in the design domain such that the output displacement is optimized i.e. maximizing the joint’s sensitivity, but their methods do not consider the other effects such as the stiffness on other axes. A flexure bearing operates by bending of materials, which causes motion at microscopic level, so friction is very uniform. For this reason, flexure bearings are often used in sensitive precision measuring equipment (see for instance [43]).

Flexure bearings benefit from a very low and very predictable friction. Many other bearings rely on sliding or rolling motions, which are necessarily uneven because the bearing surfaces are never perfectly flat. On the other hand Flexural joints have been mostly fabricated with metals that benefit usually from low young modulus and high tensile strength.

Additive manufacturing addressed the fabrication problem to some extent. Even though there exist additive manufacturing units for metals, the application of such devices for plastics and polymers is more wide spread and low cost. On the other hand the problem of their lower ratio of  $\sigma_y/E$  (yield strength/young modulus) compared to metals and thus it is important to consider and try to address this problem.  $\sigma_y/E$  is an important feature of flexural joints[44].

Smaller tensile modulus is beneficial since it reduces the required force for bending of the joints in the desired direction. However for the material to stay in its elastic zone and not entering the permanent plastic deformation, a high  $\sigma_y$  is advantageous. Lotti et. al. compared the  $\sigma_y/E$  of some materials, and based on their result they developed a single piece finger with Teflon (PTFE) material [44]. The single piece finger was developed by removal manufacturing from a single block.

In another research work the same team utilized coil springs as joint of the fingers of the previously mentioned UB-Hand [45]. Despite the fact that in the latter case the hand’s digits are not anymore composed of a single piece endoskeleton, the concept of utilization of coil springs was interesting due to the low stiffness against the flexion. However in both cases, the other aspects of joint such as undesired deflection and undesired torsion were not discussed. This aspect was later discussed in [46] in which

researchers developed a small compliant grasping mechanism with the shape deposition molding of compliant materials as joints. However, in order to reduce the undesired deflections in the fingers, they integrated a thin steel reinforcement piece into the joints. In summary, an ideal compliant joint to be used in the digits of a bionic hand or an industrial gripper should be flexible about the flexure axis and have the following characters:

- Low stiffness in the direction of the desired bending;
- High stiffness against undesired deflection and torsions;
- Lower ratio of  $\sigma_y/E$  and thus a high elastic property range.

## 4.2. Compliant joints

In this section will be discussed several possible versions of the compliant joints and their different properties as well as their fabrication. This includes joints formed by highly elastic compliant materials with and without the reinforcements, and joints formed by rigid materials.

### 4.2.1. Compliant materials - shape deposition modelling

Similar to the SDM hand [47], the first version of the ISRSofthand[31] was created with this method. Despite all benefits of elastic joints, both hands had the same disadvantage – lateral deflection. Lateral deflections are not desired in the hand since they may cause slippage after grasping the object and thus such deflection should be minimized. The lateral deflection of the elastic joints can be problematic, especially for the thumb, as can be seen in Figure 4.1. In order to have a clear idea, can be used the beam deflection model in order to estimate the joint deflection on both axes, i.e. the desired flexion and the undesired deflection. Figure 4.2 demonstrates the applied forces to the finger for a tip pinch grasp, where  $F_n$  indicates the normal force and  $F_f$  indicates the resulting tangential force. Figure 4.3 demonstrates the normal and lateral forces applied to one finger.

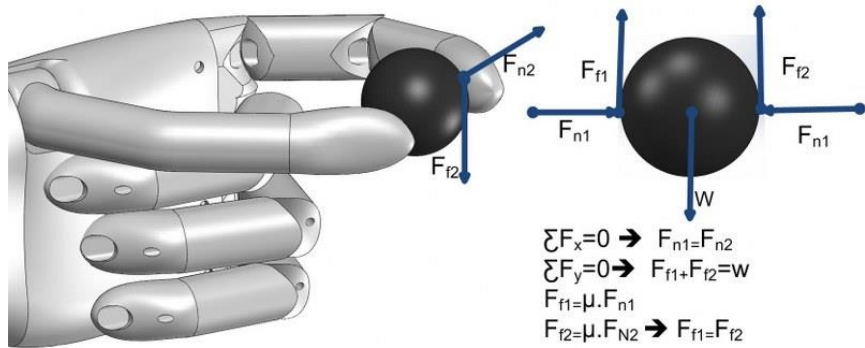


Figure 4.2 - Forces applied to the fingers in a tip pinch

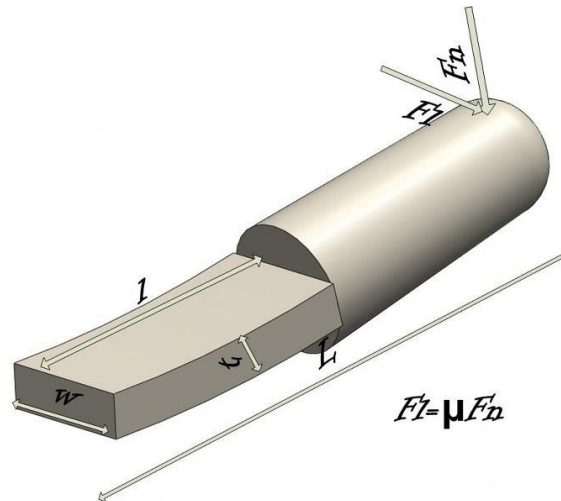


Figure 4.3 - Model of the joint bending

The deflection of the joint can be estimated by [48]:

$$\delta = \frac{Fl^3}{3EI}. \quad (4.1)$$

where  $\delta$  determines the amount of the deflection of the beam at the length of  $l$ , which is caused by a force of  $F$ , and  $E$  is the material Young's Modulus and  $I$  is moment of inertia of the beam. For a rectangular beam  $I$  is calculated as:

$$I = \frac{bh^3}{12}. \quad (4.2)$$

where  $h$  is the dimension in the plane of bending, i.e. in the axis in which the bending moment is applied. Here the inertia of the beam in the desired flexion bending is called as  $I_f$  and the inertia of the beam on the undesired lateral bending as  $I_l$ . Also  $\delta_f$  and  $\delta_l$  demonstrate the deflection on the flexion axis (desired) and lateral deflection (undesired). From Figure 4.3 we have:

$$I_f = \frac{\omega t^3}{12}. \quad (4.3)$$

$$I_l = \frac{t\omega^3}{12} \quad (4.4)$$

$$I_f = \frac{\omega t^3}{12} \quad (4.5)$$

$$I_l = \frac{t\omega^3}{12} \quad (4.6)$$

$$\delta_f = \frac{F_f L^3}{36\omega t^3} \quad (4.7)$$

$$\delta_l = \frac{F_n L^3}{36t\omega^3} \quad (4.8)$$

Thus:

$$C = \frac{\delta_l}{\delta_f} = \frac{F_f \omega t^3}{F_n t \omega^3} = \mu \left( \frac{t}{\omega} \right)^2. \quad (4.9)$$

Where C shows the ratio between the undesired lateral deflection and desired deflection, which should be minimized. At the same time, to have a stable grasp the actual amount of the undesired deflection ( $\delta_l$ ), should be limited to a predetermined value (e.g. less than 1mm). By simply increasing the thickness of the joint (t), both conditions can be satisfied. However, increasing the t results in the cubic growth of the required force for flexion of the joint in the desired direction. Therefore it is highly desirable to keep the t as low as possible.

#### 4.2.2. Reinforced joints

The other method to increase the joint stiffness against the undesired lateral deflection is to integrate into the joint a thin layer of a second material with a higher young modulus than the elastic material, and with a high  $w/t$  (width to thickness) value. If this new layer is inserted in the center of the elastic beam, and considering that its thickness is significantly smaller than the elastic material, the moment of inertia can be calculated as the sum of the moments of the inertia of both beams (for more information please refer to [48]). That is:

$$I_{fn} = I_f + \alpha \frac{\omega_r t_r^3}{12}. \quad (4.10)$$

$$I_{ln} = I_l + \alpha \frac{t_r \omega_r^3}{12} \quad (4.11)$$

In which  $I_{fn}$  and  $I_{ln}$  are the new moment of inertia of the joint against the desired flexion and the undesired lateral bending,  $w_r$  and  $t_r$  are the width and the thickness of the enforcement layer, and  $\alpha = \text{frac}(Er/Ec)$  is the ratio between the Young modulus of the integrated reinforcement and the original highly elastic material with low Young modulus. It should be noted that this model works only if the reinforcement is located in middle of the joint, since the center of mass stays unchanged in both cases (with or without reinforcement). Otherwise one needs to find out the new center of mass and recalculate the moment of inertia around the new shifted axis.

Figure 4.4 shows a model of a thumb which integrates a thin layer of reinforcement. This was applied and tested in the second version of the ISR-Softhand [31]. Despite effectively reducing the deflections, this model increased substantially the required force for closing of the thumb (this will be further analysed in the next section.) For the rest of the fingers, the problem of deflection is less significant than for the thumb, since in grasping of heavier objects, usually all 4 fingers distribute loads among all of them. Therefore, the reinforcement for the fingers were redesigned and optimized for having less stiffness in the axis of flexion, thus reducing the total power required to close the fingers.

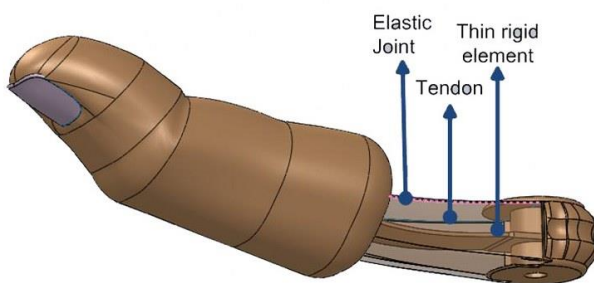


**Figure 4.4 - A thin rigid part is integrated to the thumb's flexible joint in order to increase the thumb's lateral stiffness**

### 4.3. Flexible joints through geometrical features on rigid materials

While the solution of integration of a reinforcement could reduce the deflections, it increased also the joint's stiffness and therefore the required force for closing of the finger. Hence, it is interesting to study alternatives for the reinforcement part to result in joint with lower stiffness about one axis, and high stiffness on others. It is known that for a rectangular shape reinforcement the width ( $w$ ) of the reinforcement has a cubic

relation and thus positive effect on creation of high stiffness on the other joints, and the thickness ( $t$ ) of the reinforcement increases the required force for closing of the joint by a cubic order. But the question is, how integration of non-rectangular shapes can help in creation of more optimal joints.

#### 4.3.1. Design and simulations

Thus were designed several new joints and which were simulated in terms of the desired flexion, undesired deflection and twisting, as well as the stress concentration. For the joint creation were mostly tried repeated patterns, i.e. a series of triangular, rectangular and circular patterns in which the final flexion was resulting from superposing of many small flexion for each of the patters. Several different joint were then created and simulated for early mentioned factors.

Figure 4.5 shows the model of the 8 different joints:

- A flat reinforcement, as was already used in the ISRSofthand (Sample A);
- A triangular geometry that is repeated for four times with the width of 13mm and thickness of 1mm (Sample B);
- A rectangular geometry that is repeated for four times with the width of 13mm and thickness of 1mm. After several iterations was decided to apply the fillets with radius of 1mm at some sharp edges in order to improve the characteristics of the joint (Sample C);
- A circular geometry that is repeated for four times with the width of 10mm and thickness of 1mm (Sample D);
- Same geometry of the above with the width of 15mm and 13mm (Sample E and Sample H (tested only with FEA) respectfully);
- A circular pattern with a different geometry from (D) to analyse the effect of the geometry (Sample G).

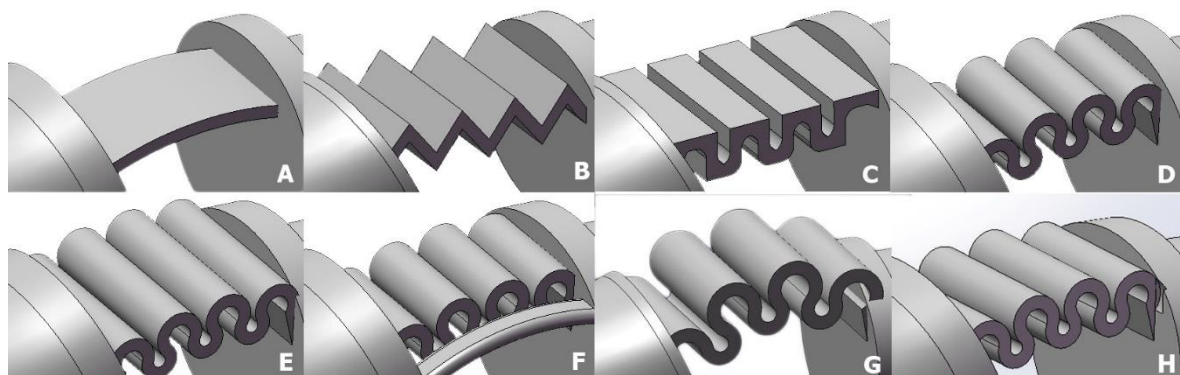


Figure 4.5 - Different joint models used for tests

At the Figure 4.6 can be observed a different geometries used in samples D/E/H and G:

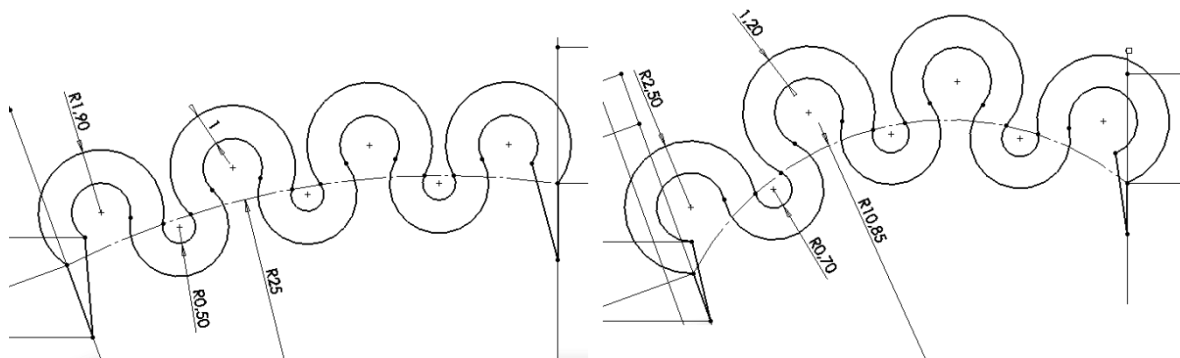
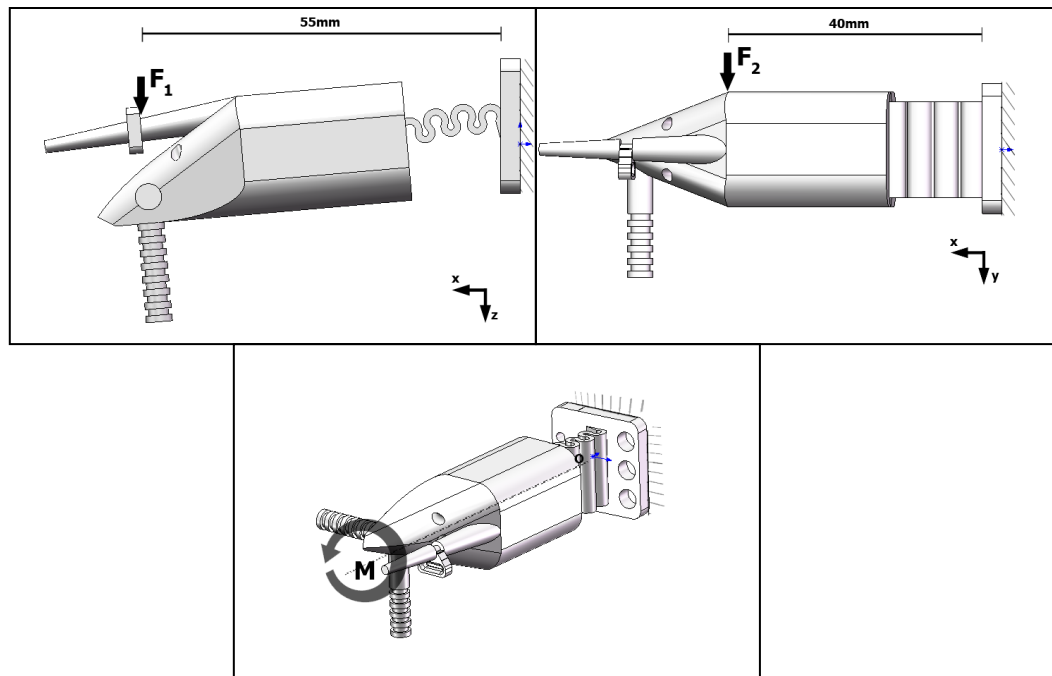


Figure 4.6 - Geometry used in circular pattern joints D, E H (left) and G (right)

Except the flat geometry, it is difficult to use analytical models for calculation of these joint's deflection. Therefore a FEA (Finite Element Analysis) was used, in order to compare several characteristics of the joints. A non-linear analysis for large deformations was performed using a Solidworks Simulation software. Previous tests with the real models were performed to determinate an optimal load value that will not damage the models but will be large enough for taking measurements with good precision during experimental measurement. A torque, applied for measuring a displacements during a twisting was calculated by multiplying a force of 5N (the reaction force on the tip of the finger after applying a load of 1kg on the hand) by a distance to the axis of the rotation. So, for each of the joints the simulations were performed for the following loads:

- Constant force ( $F_1$ ) of 0,8N acting on a Z direction applied at the distance of 0,055m from the fixed base to measure the maximum bending at the joint (Figure 4.7 top left);

- Constant force ( $F_2$ ) of 4N acting on a Y direction applied at the distance of 0,04m from the fixed base to simulate the lateral deflection (Figure 4.7 top right);
- For twisting was applied a constant torque ( $M$ ) of 0,12 N.m (Figure 4.7 bottom).



**Figure 4.7 - Three types of loads analysed during FEA, maximum bending (top left), lateral deflection (top right) and displacement due to torsion (bottom)**

In all simulations were considered the properties of the materials produced by a SLS 3D printer, from a worldwide additive manufacturing service provider.

As also stated in [44], the choice of material is very important because achievement of high strain without overcoming the yield strength requires a material with a high  $\sigma_y/E$  ratio. In [44], authors calculated this ratio for several plastics and metals, and found out that PTFE, has a very good  $\sigma_y/E$  ratio of 66.7 compared to 7.1 in Aluminum 7075. Here was made the same comparison between the 3D printed methods and materials, in order to find out the best solution.

**Table 4.1 - Comparison between the  $\sigma_y/E$  ratio of 3D printed materials [49]**

Material/Methods	Yield Strength $\sigma_y$ (MPa)	Young's modulus, E (MPa)	$\sigma_y/E \times 1000$
Polyamide/SLS	48	1700	28
Resin example/SLA	26	1100	23
Alumide/SLS	48	3800	12

ABS/FDM	36	2265	16
---------	----	------	----

Table 4.1 compares only the mostly used 3D printed materials, and properties of these materials are selected from a large 3D printing service provider. As can be seen in Table 4.1, a polyamide material that is produced with SLS (Selective laser sintering of a powder), has the best  $\sigma_y/E$  ratio. With 3D printing methods, not only the material is important, but also the production method makes a difference on the properties of the material, since these properties depends on the density of the object and bonding between the layers. Considering that the 3D printed parts are generally inferior in properties compared to a machined plastic block, the  $\sigma_y/E$  value (28) of the polyamide 3D printed parts seems to be good enough compared to the list of materials provided in Table 4.1. Therefore this material was used for prototyping of the fingers.

#### 4.3.2. Experimental setup

In order to validate the results of the simulations, some fingers were 3D printed as a test benchmark in order to compare them with the simulation results. As can be seen in Figure 4.8, test model includes a flexible joint (1), a rigid part (2), two perpendicular bars (3) which are designed to add a mass, in order to simulate the deflection and torsion of the joint in different directions, a sharp tip (4) used for taking the measurements and a base (5) with screw holes for fixing the model.

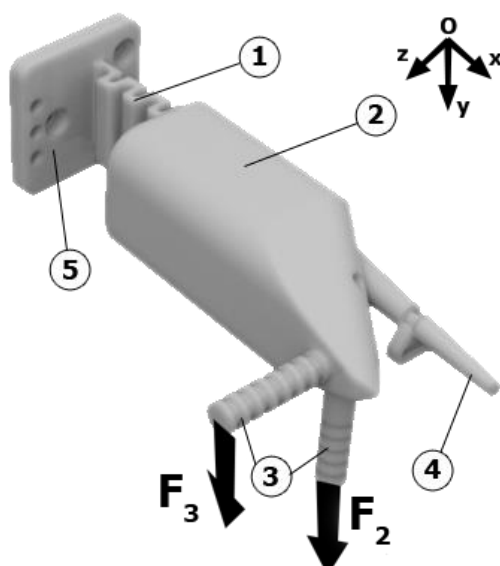


Figure 4.8 - A model of an example finger for a tests

In the experimental setup, it wasn't possible to simulate the pure torsion as it was simulated in the simulation software, because the added mass would cause a torsion accompanied by a lateral deflection. In any case, this is actually what happens in the actual grasping, i.e. a tangential force is applied to the fingers that causes the deflection and the torsion at the same time.

Figure 4.9 shows all test models together. In the next section the results of the simulation and the experimental setup will be presented and discussed.



Figure 4.9 - Experimental setup for measuring an undesired deflection

#### 4.4. Results and discussion

For the best functionality of the joints, it is desired to minimize the lateral deflection and also the torsion of the joint due to lateral forces. But it is also desirable to have the minimum bending force for flexion of the joint. Two new criteria were created then:

“ $LD/FL$ ” denotes for the amount of the lateral deflection (displacement in mm) divided by the amount flexion (displacement in mm). Also the “ $Tor/FL$ ” which determines the amount of the displacement due to the torsion divided by the displacement due to the flexion. Both values should be minimum. While these are unit-less ratios, should be noted that the displacement due to flexion should be also as high as possible.

#### 4.4.1. Simulation results

During the FEA a curvature based mesh was used. With a curvature based mesh, the size of each mesh element is determined mathematically by the minimum number of elements that fit in a hypothetical circle, while taking into account the user specified minimum and maximum element size. For all models the same values for minimum and maximum element sizes of 0,6mm and 3,0mm respectfully were applied. As a result, due to the differences in a joint geometries, the number of mesh elements is different for each model and is placed in the range between 35000 and 45000 elements.

On the Figure 4.10 and Figure 4.11 can be visualized the results for undesired lateral deflection and displacement due to torsion respectfully obtained after FEA for one of the sample joins (Sample C). Results for all tested joint are shown at the Table 4.2.

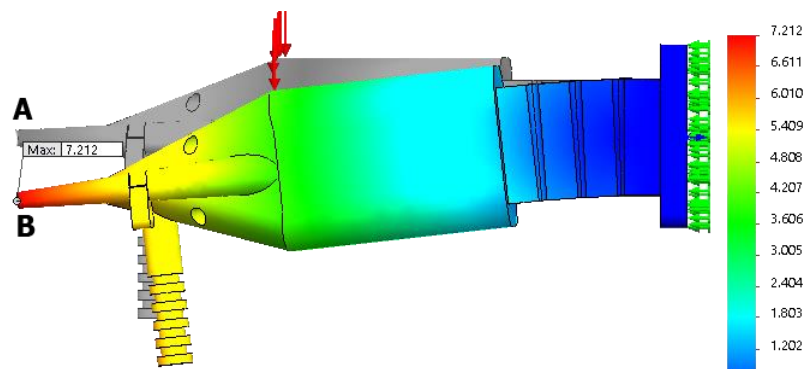


**Figure 4.10 - Displacement visualization after FEA for lateral displacement. A - initial position, B - final position**

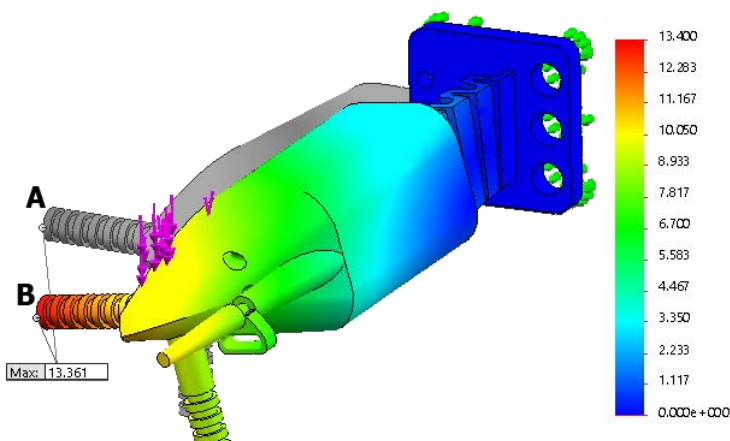


**Figure 4.11 Displacement visualization after FEA for torsion. A - initial position, B - final position**

**Table 4.2 - Simulation results, the lateral deflection is measured after applying a constant force of 4N (F2) on all samples. The right column shows the total displacement on the tip of fingers after application of a torsional torque (M) of 0,12N.m**

	Lateral deflection, mm	Displacement due to torsion, mm
Sample A	2,3	46,0
Sample B	3,7	26,5
Sample C	5,0	13,4
Sample D	21,7	38,6
Sample E	7,6	19,4
Sample F	1,1	19,7
Sample G	9,1	17,4
Sample H	11,2	22,4

FEA results for maximum bending can be observed at the Table 4.3, which also shows two unit-less ratios defined in the beginning of this chapter,  $LD/FL$  and  $Tor/FL$ .

**Table 4.3 - Simulation results, 2nd column shows maximum bending displacement, 3rd shows a ratio between lateral deflection (LD) and displacement due to flexion (FL) and 3rd column shows a ratio between displacement due to torsion (Tor) and FL**

	Flexion, mm	LD/FL	Tor/FL
Sample A	22,5	0,10	2,04
Sample B	22,2	0,17	1,19
Sample C	21,2	0,24	0,63
Sample D	37,3	0,58	1,04
Sample E	27,6	0,28	0,70
Sample F	18,3	0,06	1,08
Sample G	21,2	0,43	0,82
Sample H	30,9	0,36	0,72

A maximum stress value that occurs in every joint is shown at the Table 4.4. Results for von Miss equivalent for stress distribution during bending are displayed at the Figure 4.12.

**Table 4.4 - Simulation results, maximum stress value for each type load**

	Flexion, MPa	Lateral Deflection, MPa	Torsion, MPa
Sample A	24,8	18,9	142,9
Sample B	17,7	13,8	63,5
Sample C	18,4	54,5	79,8
Sample D	29,2	95,7	179,0
Sample E	21,7	52,5	138,5
Sample F	25,7	25,1	114,4

Sample G	15,8	42,0	86,5
Sample H	23,6	68,1	146,4

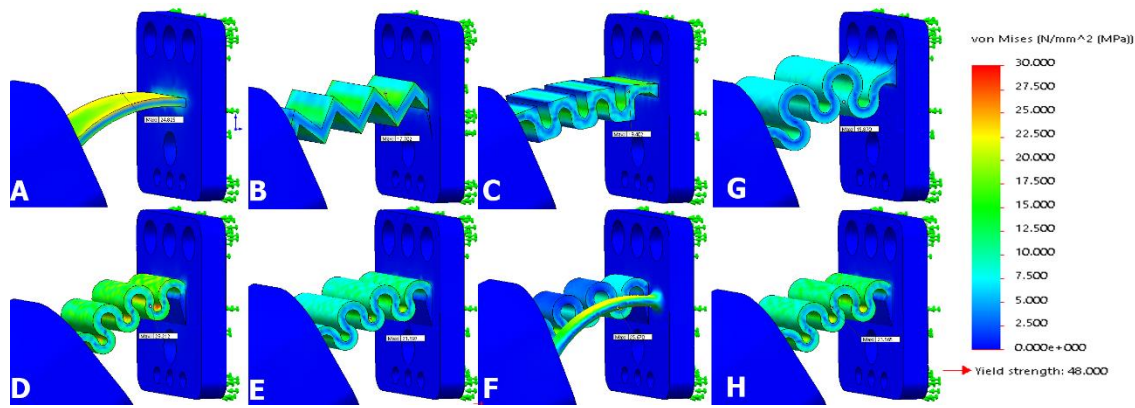


Figure 4.12 – Von Miss equivalent for stress distribution in each joint after FEA of applying a load  $F_1 = 0,8\text{N}$  for maximum bending test

#### 4.4.2. Experimental results

For better interpretation of joint behaviour two different loads were applied: 150g and 300g for undesirable deflections. A displacement second two axes was measured and then a total displacement,  $\delta$ , was obtained by calculating a length of obtained vector. The same method was used to measure a desired displacement (Flexion) with masses of 40g and 80g.

For the best functionality of the joints, it is desired to minimize the lateral deflection and also the torsion of the joint due to lateral forces. But it is also desirable to have the minimum bending force for flexion of the joint.

Table 4.5 shows the results of the undesired deflections for two different masses of 150gr and 300gr applied in the direction of “ $F_2$ ” and “ $F_3$ ” (Figure 4.8). The amount of the flexion on each of the joints when a mass of 40g and 80g is applied in the direction of  $F_1$  (Figure 4.7, top left) as well as  $LD/FL$  and  $Tor/FL$  ratios are displayed at the Table 4.6. Here, higher deflections are desired. Higher deflection means that the joint offers less resistance against the flexion.

Table 4.5 - Experimental results for undesirable deflection

		$m_1 = 150\text{g}$		$m_2 = 300\text{g}$	
		Lateral deflection	Displacement due to torsion	Lateral deflection	Displacement due to torsion
Sample A	y, mm	0,0	4,8	0,0	18,3
	z, mm	1,2	2,4	3,8	13,0
	$\delta$ , mm	<b>1,2</b>	<b>5,4</b>	<b>3,8</b>	<b>22,4</b>

Sample B	y, mm	0,0	2,9	0,0	7,3
	z, mm	5,2	6,4	11,3	14,9
	$\delta$ , mm	<b>5,2</b>	<b>7,0</b>	<b>11,3</b>	<b>16,6</b>
Sample C	y, mm	0,0	-2,2	0,0	2,2
	z, mm	5,9	5,8	12,3	12,5
	$\delta$ , mm	<b>5,9</b>	<b>6,2</b>	<b>12,3</b>	<b>12,6</b>
Sample D	y, mm	0,0	-6,7	0,0	8,9
	z, mm	20,0	19,7	32,0	32,9
	$\delta$ , mm	<b>20,0</b>	<b>20,8</b>	<b>32,0</b>	<b>33,5</b>
Sample E	y, mm	0,0	1,5	0,0	14,9
	z, mm	9,6	9,0	15,3	2,1
	$\delta$ , mm	<b>9,6</b>	<b>9,1</b>	<b>15,3</b>	<b>14,1</b>
Sample F	y, mm	0,0	3,0	0,0	22,0
	z, mm	1,8	2,7	2,4	9,5
	$\delta$ , mm	<b>1,8</b>	<b>4,0</b>	<b>2,4</b>	<b>24,0</b>
Sample G	y, mm	0,0	2,7	0,0	5,4
	z, mm	10,4	9,4	18,4	18,2
	$\delta$ , mm	<b>10,4</b>	<b>9,8</b>	<b>18,4</b>	<b>18,9</b>

**Table 4.6 - Desired displacement, the ratios between lateral deflection (LD) and displacement due to flexion (FL) and the ratios between displacement due to torsion (Tor) and FL. All ratios were calculated using the results of displacement values for higher masses, m2 and m4**

		Flexion		LD/FL	Tor/FL
		m <sub>3</sub> = 40g	m <sub>4</sub> = 80g		
Sample A	y, mm	8	15	0,16	0,85
	z, mm	10,8	18,2		
	$\delta$ , mm	<b>13,4</b>	<b>23,6</b>		
Sample B	y, mm	10,4	20,2	0,41	0,56
	z, mm	12,1	18,3		
	$\delta$ , mm	<b>16,0</b>	<b>27,3</b>		
Sample C	y, mm	8,7	17,3	0,42	0,40
	z, mm	14,6	23,5		
	$\delta$ , mm	<b>17,0</b>	<b>29,2</b>		
Sample D	y, mm	17,2	27,5	0,96	0,95
	z, mm	15,3	19,1		
	$\delta$ , mm	<b>23,0</b>	<b>33,5</b>		
Sample E	y, mm	10,4	20,8	0,50	0,44
	z, mm	14,9	22		
	$\delta$ , mm	<b>18,2</b>	<b>30,3</b>		
Sample F	y, mm	7,6	12,6	0,11	0,97
	z, mm	11,2	18		
	$\delta$ , mm	<b>13,5</b>	<b>22,0</b>		
Sample G	y, mm	7,6	14,8	0,74	0,71

	<b>z, mm</b>	13,4	20,1		
	<b>δ, mm</b>	<b>15,4</b>	<b>25,0</b>		

With a purpose to compare the results obtained by FEA and experimental results, a chart was made, where were faced results for common for both analyses criteria “LD/FL”. As can be observed from the Figure 4.13, there is a pattern in which the values of “LD/FL” are increasing or decreasing is same for both simulation and experimental results. That is an increase on this value in the simulation, is always confirmed in the experimental results. For instance sample F – has the lowest value, D – is the highest, B and C are similar in both studies. However the exact values of “LD/FL” are different in simulation and experimental results. This might be due to several reasons, such as defects during 3D printing, layer inconsistencies and the fact that 3D printing results in an anisotropic part, which weren't predicted by FEA.

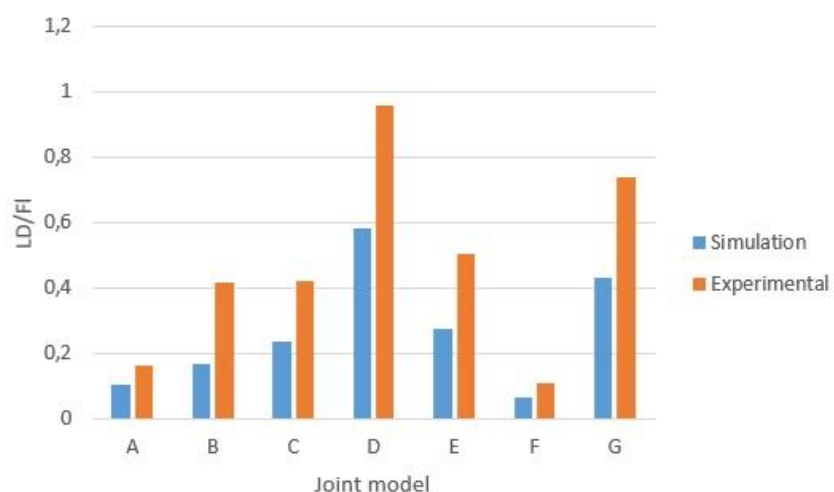


Figure 4.13 - Comparison between the results for "LD/FL" obtained by FEA and experimental methods

#### 4.5. Creation of the hand's digits

Based on tests performed with the ISR-Softhand at [31], was found out that the thumb should have the highest stiffness against lateral deflection and undesired twisting, since it is suffering higher tangential and normal forces than the other fingers. That is, to grasp a heavy object the thumb should oppose the force that on the other side is divided by the other 4 fingers. For other fingers, such stiffness can be lower, in favour of lower required force for full flexion of the fingers, in order to reduce the required power for closing of the fingers. Therefore in the next version of the hand, to replace the conventional shafted IP joint, will be used the joint of the "C" configuration for the thumb, and the "D"

configuration joint will be used in place of PIP joint in the other fingers. Was decided to maintain a shafted configuration of MCP joint for this finger version in order to decrease an overall lateral deflection.

Figure 4.14 shows the fabrication method for the finger: a one piece 3D printed endoskeleton is placed in a mold which then is filled by a silicon material Ecoflex® 00-30 with a very low Young modulus. Since the enveloping polymer benefits from a low Young modulus, it can fill the joint without having a significant effect on the joint behaviour. The soft enveloping polymer has an important roles on formation of larger contact areas and a high friction coefficient, and thus a more stable grasp.



**Figure 4.14 - Fabrication of a compliant finger, a 3D printed endoskeleton inserted into the designed mold which then filled with a silicone resin**



## 5. CONCLUSIONS

### 5.1. General conclusions

A custom-made upper-limb prosthetic device was designed, fabricated and tested in order to deliver it for an 8-year boy with right hand disorder. A special attention was given to develop such characteristics as light weight, low cost and intuitive control - a valuable characteristics for the adult prosthetics, which becomes essential for children. The recent advancements in additive manufacturing technologies played a crucial role in achievements of proposed objectives.

The final design was based on a concept spread in a last years by a worldwide community e-Nable Group. Major upgrades were made relatively available designs which improve significantly a usability of a prosthesis. Despite the device was customized for an individual person, it can be easily modified to fit people with other kind of hand disorders and fulfil their necessities. The contributions of this works will enable a great breakthrough in development of better low cost open source actuator-less prosthetic terminals.

During this research work, the new design for compliant joints was developed. A common problem of undesired lateral deflections was partially solved by integrating of repetitive flexural joints into the joints geometry. A 3D printed endoskeleton is involved by a silicon material, Ecoflex® 00-30, which gives a final form to the finger. This feature has an important role on formation of larger contact areas and a high friction coefficient and thus a safer and more stable grasp. In addition a more anthropomorphic look is given to the hand. Contributions compared to the state of the art enable hands can be summarized as:

1. The thumb's position;
2. The rigid support with a compliance layer on the palm as additional contact point;
3. The compliant fingers with high friction silicon cover.

### 5.2. Future works

In a brief future we plan to make this prosthesis model available for free at different web platforms, including an e-Nabled group [9] so it can be built by other people

---

and delivered for someone in need. Also, we will prepare a tutorial that would be available for the e-Nable community for fabrication of this version of the hand. The other purpose of sharing this model is for the developed in this research work features can be used by other researchers and designers in their developing processes, as the “Cyborg Beast” hand was used for the purpose of this work.

Although this model has fulfilled a proposed for this work objectives, there is always a space for improvements. Some of them are already planned for the next versions of the hand.

We showed that big variety of objects can be handled by the last version of the prosthesis. In order to increase a number of possible grasps, adding an articulation that allows the thumb to change manually between abducted and adducted positions is planned for next versions of the device, as well as adding a locking mechanism to the finger sockets that will allow to use hook grasp for heavier objects. Improving an esthetical appearance of the device by making it look more like a human hand is also planned for the next versions of the prosthesis.

Another future research plan is to increase the range of usability of the compliant joint. Integrating it into an active prosthetic hands and industrial soft grippers are possible ways to do it.

### **5.3. Publications**

Andiy Sayuk, Mahmoud Tavakoli, Pedro Neto “Compliant joints with rigid materials: additive manufacturing of geometrical features for the applications of grasping”, submitted for possible publication in “ASME journal of Mechanisms and Robotics”.

## BIBLIOGRAPHY

- [1] P. De Leva, “Adjustments to zatsiorsky-seluyanov’s segment inertia parameters,” *J. Biomech.*, vol. 29, no. 9, pp. 1223–1230, 1996.
- [2] C. Pylatiuk, S. Schulz, and L. Döderlein, “Results of an Internet survey of myoelectric prosthetic hand users.,” *Prosthet. Orthot. Int.*, vol. 31, no. 4, pp. 362–70, Dec. 2007.
- [3] WorkSafeBC Evidence-Based Practice Group and Dr. Craig W. Martin, “Upper Limb Prostheses A Review of the Literature With a Focus on Myoelectric Hands,” *Clin. Serv. – Work. Empl. Serv.*, no. February, 2011.
- [4] M. Egermann, P. Kasten, and M. Thomsen, “Myoelectric hand prostheses in very young children.,” *Int. Orthop.*, vol. 33, no. 4, pp. 1101–5, Aug. 2009.
- [5] I. Dudkiewicz, R. Gabrielov, I. Seiv-Ner, G. Zelig, and M. Heim, “Evaluation of prosthetic usage in upper limb amputees.,” *Disabil. Rehabil.*, vol. 26, no. 1, pp. 60–3, Jan. 2004.
- [6] E. A. Biddiss and T. T. Chau, “Multivariate prediction of upper limb prosthesis acceptance or rejection.,” *Disabil. Rehabil. Assist. Technol.*, vol. 3, no. 4, pp. 181–92, Jul. 2008.
- [7] H. Bouwsema, C. K. Van Der Sluis, and R. M. Bongers, “Guideline for training with a myoelectric prosthesis,” no. July, 2013.
- [8] H. Bouwsema, C. K. Van Der Sluis, and R. M. Bongers, “Learning to control opening and closing a myoelectric hand,” *Arch. Phys. Med. Rehabil.*, vol. 91, no. 9, pp. 1442–1446, 2010.
- [9] “E-Nabling The Future.” [Online]. Available: <http://enablingthefuture.org/>. [Accessed: 01-Jan-2015].
- [10] “Dad Uses 3D Printer To Make His Son A Prosthetic Hand,” *Huffington Post*, 11-Apr-2013.
- [11] “BeBeonic Hand.” [Online]. Available: [http://bebionic.com/the\\_hand](http://bebionic.com/the_hand).
- [12] “I-Limb hand.” [Online]. Available: <http://www.touchbionics.com/products>.
- [13] “Vincent Systems GmbH.” [Online]. Available: <http://vincentsystems.de/en/>. [Accessed: 01-Jan-2015].

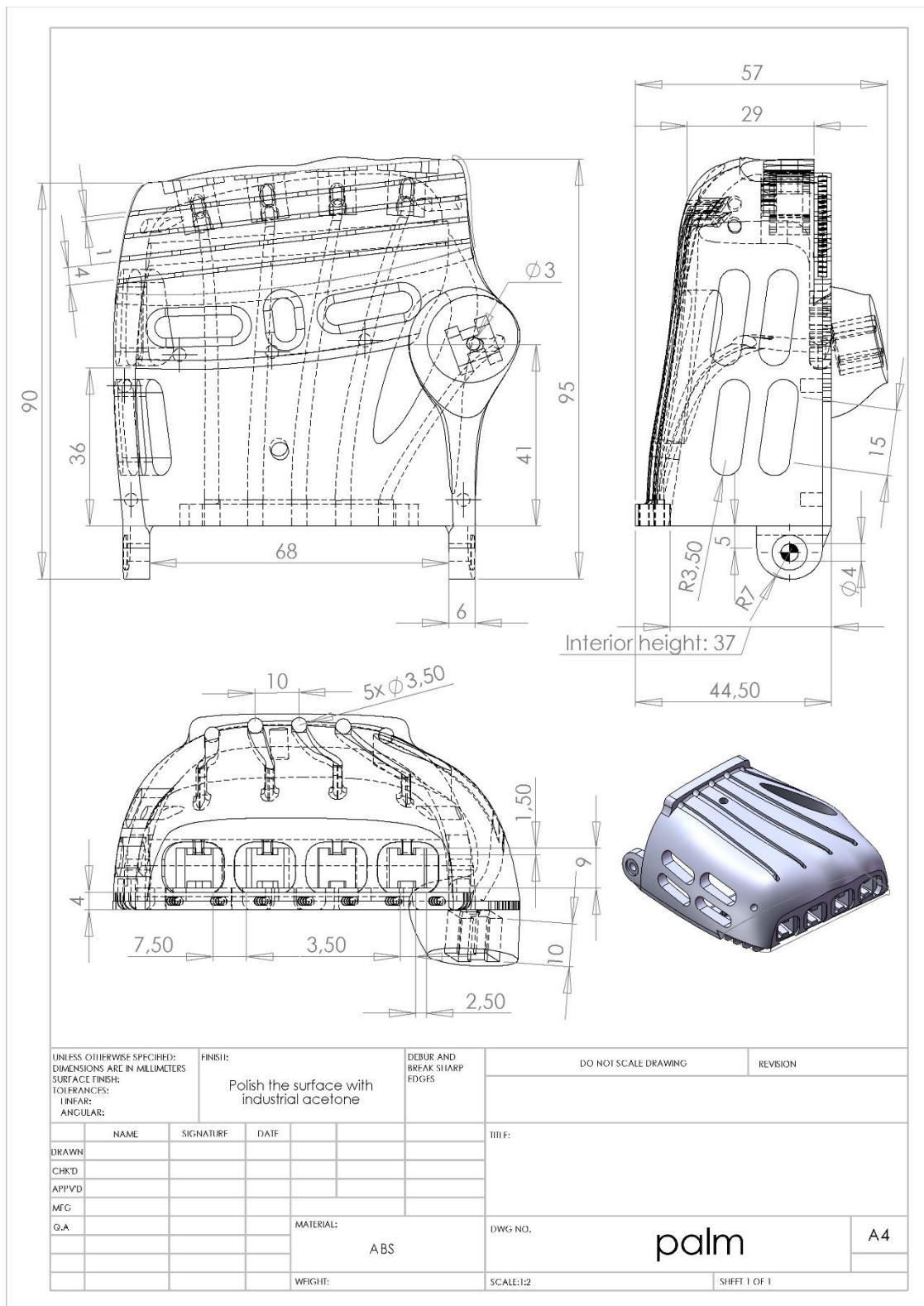
- [14] “MICHELANGELO PROSTHETIC HAND.” [Online]. Available: <http://www.hangerclinic.com/limb-loss/adult-upper-extremity/adv-tech/Pages/Michelangelo-Hand.aspx>. [Accessed: 01-Sep-2015].
- [15] “KifidisOrthopedics.” [Online]. Available: [www.kifidis-orthopedics.gr](http://www.kifidis-orthopedics.gr). [Accessed: 01-Aug-2015].
- [16] “Transplant patient receives bionic hand with electronic fingers.” [Online]. Available: <http://www.telegraph.co.uk/news/science/science-news/9820605/Transplant-patient-receives-bionic-hand-with-electronic-fingers.html>. [Accessed: 28-Aug-2015].
- [17] M. S. Charles M. Fryer, B.S. and C. P. O. John W. Michael, M.Ed., “Upper-Limb Prosthetics: Body-Powered Components,” in *Atlas of Limb Prosthetics: Surgical, Prosthetic, and Rehabilitation Principles*, 2nd ed., American Academy of Orthopedic Surgeons, 1992.
- [18] “Hosmer Hooks.” [Online]. Available: <http://hosmer.com/products/hooks/index.html>. [Accessed: 01-Aug-2015].
- [19] “Amputee Supply.” [Online]. Available: <http://www.amputeesupply.com/>.
- [20] “Otto Bock - System Hand.” [Online]. Available: [http://www.ottobock.com/cps/rde/xchg/ob\\_com\\_en/hs.xsl/3733.html](http://www.ottobock.com/cps/rde/xchg/ob_com_en/hs.xsl/3733.html).
- [21] F. Rengier, A. Mehndiratta, H. von Tengg-Kobligk, C. M. Zechmann, R. Unterhinninghofen, H.-U. Kauczor, and F. L. Giesel, “3D printing based on imaging data: review of medical applications.,” *Int. J. Comput. Assist. Radiol. Surg.*, vol. 5, no. 4, pp. 335–41, Jul. 2010.
- [22] J. Gibbard, “Dextrus Hand.”
- [23] E. Innes, “The 3D printed hand that could change the world,” *14 October 2013*, 2013. [Online]. Available: <http://www.dailymail.co.uk/health/article-2458572/The-Dextrus-3D-printed-prosthetic-hand-Graduate-creates-600-robotic-limb-change-world.html>. [Accessed: 01-Aug-2015].
- [24] N. E. Krausz, R. a L. Rorrer, and R. F. Weir, “Design and Fabrication of a Six Degree-of-Freedom Open Source Hand,” vol. 4320, no. c, pp. 1–9, 2015.
- [25] A. Schmitz, U. Pattacini, F. Nori, L. Natale, G. Metta, and G. Sandini, “Design, realization and sensorization of the dexterous iCub hand,” in *2010 10th IEEE-RAS International Conference on Humanoid Robots*, 2010, pp. 186–191.
- [26] J. Zuniga, D. Katsavelis, J. Peck, J. Stollberg, M. Petrykowski, A. Carson, and C. Fernandez, “Cyborg beast: a low-cost 3d-printed prosthetic hand for children with upper-limb differences,” *BMC Res. Notes*, vol. 8, no. 1, 2015.

- [27] S. Wood, “Flexy Hand 2,” 2014. [Online]. Available: <http://www.thingiverse.com/thing:380665>.
- [28] J. Butterfass, M. Grebenstein, H. Liu, and G. Hirzinger, “DLR-Hand II: next generation of a dexterous robot hand,” in *Proceedings 2001 ICRA. IEEE International Conference on Robotics and Automation (Cat. No.01CH37164)*, 2001, vol. 1, pp. 109–114.
- [29] MekaBot, “Meka H2 Compliant Hand Datasheet,” 2009.
- [30] S. B. Godfrey, A. Ajoudani, M. Catalano, G. Grioli, and A. Bicchi, “A synergy-driven approach to a myoelectric hand.,” *IEEE Int. Conf. Rehabil. Robot.*, vol. 2013, p. 6650377, Jun. 2013.
- [31] M. Tavakoli, “Adaptive under-actuated anthropomorphic hand : ISR-SoftHand,” no. Iros, pp. 1629–1634, 2014.
- [32] C. Melchiorri, G. Palli, G. Berselli, and G. Vassura, “Development of the UB Hand IV: Overview of Design Solutions and Enabling Technologies,” *IEEE Robot. Autom. Mag.*, vol. 20, no. 3, pp. 72–81, Sep. 2013.
- [33] M. Tavakoli, L. Marques, and A. T. de Almeida, “Flexirigid, a novel two phase flexible gripper,” in *2013 IEEE/RSJ International Conference on Intelligent Robots and Systems*, 2013, pp. 5046–5051.
- [34] A. M. Dollar and R. D. Howe, “The Highly Adaptive SDM Hand: Design and Performance Evaluation,” *Int. J. Rob. Res.*, vol. 29, no. 5, pp. 585–597, Feb. 2010.
- [35] J. Zuniga, “Cyborg Beast Research.” [Online]. Available: <http://www.cyborgbeast.org/research/>.
- [36] L. Resnik, “Development and testing of new upper-limb prosthetic devices: research designs for usability testing.,” *J. Rehabil. Res. Dev.*, vol. 48, no. 6, pp. 697–706, Jan. 2011.
- [37] C. Luke, “The Difference Between ABS and PLA for 3D Printing,” 2013. [Online]. Available: <http://www.protoparadigm.com/news-updates/the-difference-between-abs-and-pla-for-3d-printing/>.
- [38] T. Feix, J. Romero, H. Schmiedmayer, A. M. Dollar, and D. Kragic, “The GRASP Taxonomy of Human Grasp Types.”
- [39] “Gripper Box 3.0.” [Online]. Available: <http://forums.enablingthefuture.org/viewtopic.php?f=18&t=110>. [Accessed: 01-Jan-2015].

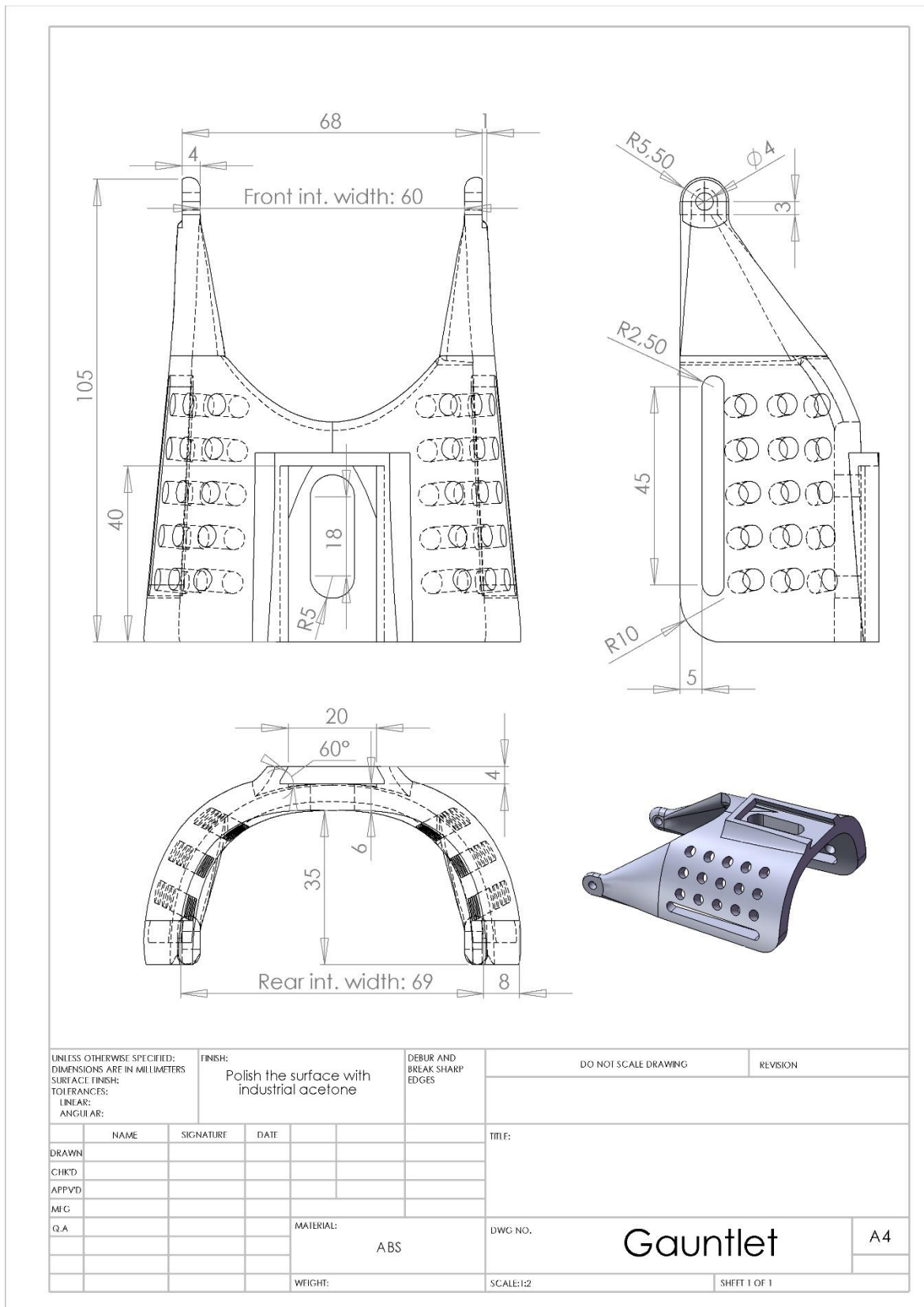
- [40] I. M. Bullock, J. Z. Zheng, S. De La Rosa, C. Guertler, and A. M. Dollar, “Grasp frequency and usage in daily household and machine shop tasks,” *IEEE Trans. Haptics*, vol. 6, no. 3, pp. 296–308, 2013.
- [41] O. Sigmund, “Mechanics of Structures and Machines : An International On the Design of Compliant Mechanisms Using Topology Optimization On the Design of Compliant Mechanisms Using Topology Optimization \*,” no. May 2015, pp. 37–41, 2007.
- [42] H. Search, C. Journals, A. Contact, M. Iopscience, and I. P. Address, “A two-stage topological optimum design for monolithic compliant microgripper integrated with flexure hinges,” vol. 840.
- [43] M. Balucani and N. P. Belfiore, “MEMS-Based Conjugate Surfaces Flexure Hinge,” vol. 137, no. January, pp. 1–10, 2015.
- [44] F. Lotti and G. Vassura, “A Novel Approach to Mechanical Design of Articulated Fingers for Robotic Hands,” pp. 2–7.
- [45] F. Lotti, P. Tiezzi, G. Vassura, L. Biagiotti, G. Palli, and C. Melchiorri, “Development of UB Hand 3: Early Results,” in *Proceedings of the 2005 IEEE International Conference on Robotics and Automation*, pp. 4488–4493.
- [46] J. Gafford, A. Harris, T. Mckenna, and D. Holland, “Shape Deposition Manufacturing of a Soft , Atraumatic , Deployable Surgical Grasper,” pp. 1–43.
- [47] A. M. Dollar and R. D. Howe, “A robust compliant grasper via shape deposition manufacturing,” *IEEE/ASME Trans. Mechatronics*, vol. 11, no. 2, pp. 154–161, 2006.
- [48] J. M. Gere, *Mechanics of Materials*. 2004.
- [49] “3D Printing Materials | Stratasys.” [Online]. Available: <http://www.stratasys.com/materials>. [Accessed: 29-Aug-2015].

# APPENDIX

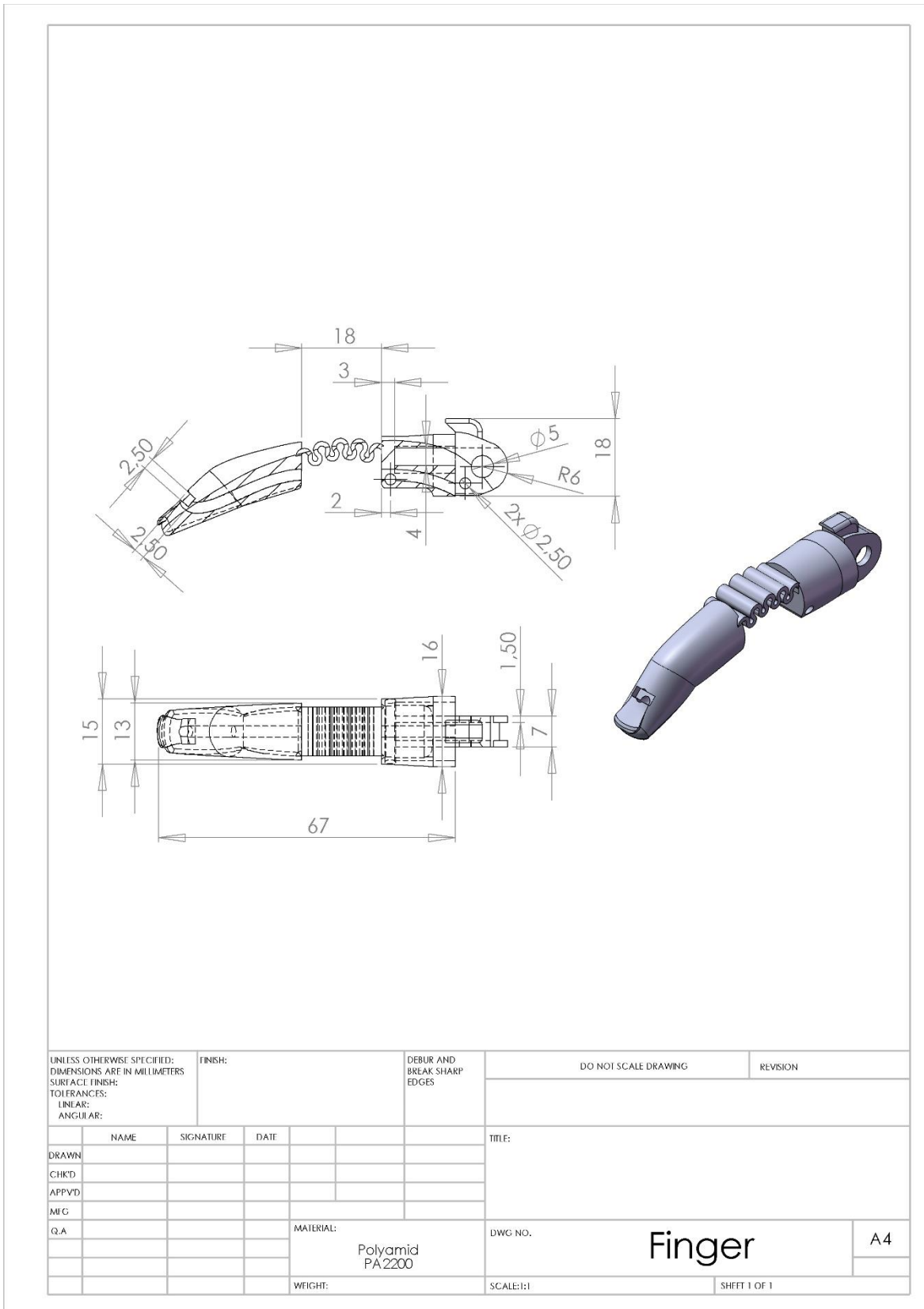
## A1. Palm Drawing



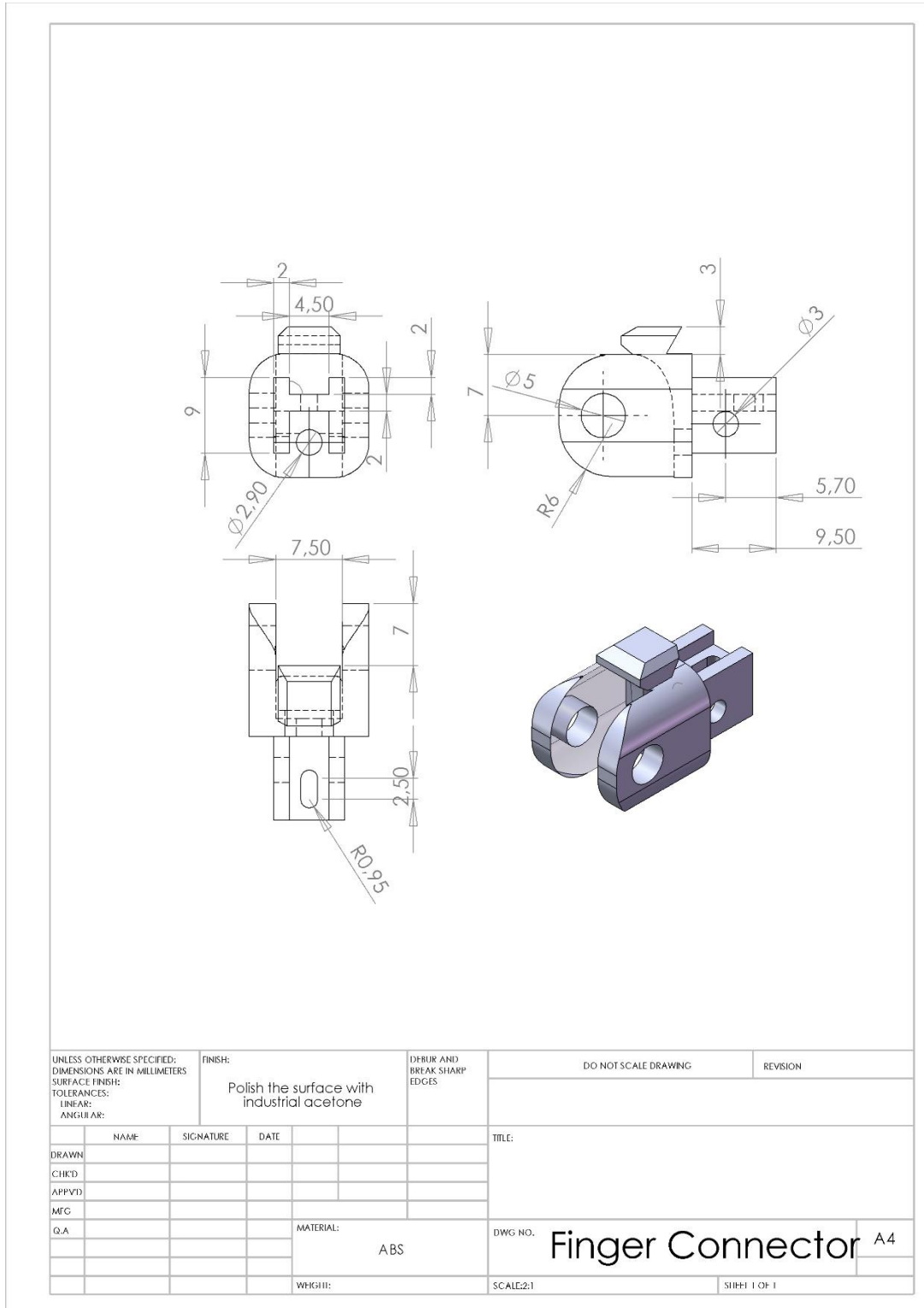
## A2. Gauntlet drawing



### A3. Finger drawing



## A4. Finger connector drawing



## A5. Detailed representations of grasps performed by Soft-Enabled Hand

Synergy	Object	Hold	Soft-Enabled Hand	Comment
1. Large diameter	Tube, d=75mm	+		
2. Small Diameter	Tube2, d=35mm	+		
3. Medium Wrap	Glass, d=58mm	+		
4. Adducted thumb		-	-	Impossible to perform with thumb in the abducted position
5. Light Tool	Pen, d=10mm	+/-		
6. Prismatic 4 finger	Pen, d=10mm	+/-		
7. Prismatic 3 Finger	Pen, d=10mm	+		Possible, if the tension of a thumb tendon cord is adjusted for the purpose
8. Prismatic 2 Finger	Pen, d=10mm	+		Possible, if the tension of a thumb tendon cord is adjusted for the purpose

9. Palmar Pinch 	Battery, d=14mm	+/-		
10. Power disk 	CD, d=120mm	+		
11. Power sphere 	Tennis ball, d=65mm	+		
12. Precision disk 	CD, d=120mm	+		
13. Precision Sphere 	Tennis ball, d=65mm	+		
14. Tripod 	Ping- pong ball, d=38mm	+		
15. Fixed Hook 	Tube2, d=36mm	+/-		

16. Lateral 	-	-	-	Impossible to perform with thumb in the abducted position
17. Index Finger Extension 	Tube2, d=36mm	+/-		Possible, but the grasp is unstable
18. Extension Type 	Plate	+		
19. Distal Type 	Scissors	+/-		
20. Writing Tripod 	-	-	-	Not possible to perform
21. Tripod Variation 	-	-	-	Not possible to perform
22. Parallel Extension 	-	-	-	Not possible to perform
23. Abduction Grip 	-	-	-	Not possible to perform without an abd./add. movement between the index and middle fingers

24. Tip Pinch 	Hex key	+		Grasp become more stable if tendons are adjusted for the purpose
25. Lateral Tripod 	Battery, d=14mm	+		
26. Sphere 4 Finger 	Tennis ball, d=65mm	+		
27. Quadpod 	Ping- pong ball, d=38mm	+		
28. Sphere 3 Finger 	Tennis ball, d=65mm	+		

29. Stick		-	-	Not possible to perform
30. Palmar		-	-	Impossible to perform with thumb in the abducted position
31. Ring	Tube, d=75mm	+		
32. Ventral		-	-	Not possible to perform
33. Inferior Pincer	Sphere, d=59mm			